KERNFORSCHUNGSANLAGE JÜLICH GmbH
Institut für Reaktorwerkstoffe

PLASTICITY – A LIMITING CASE OF CREEP

by

H. Cords, G. Kleist, R. Zimmermann

Jül-Spez-379
November 1986
ISSN 0343-7639

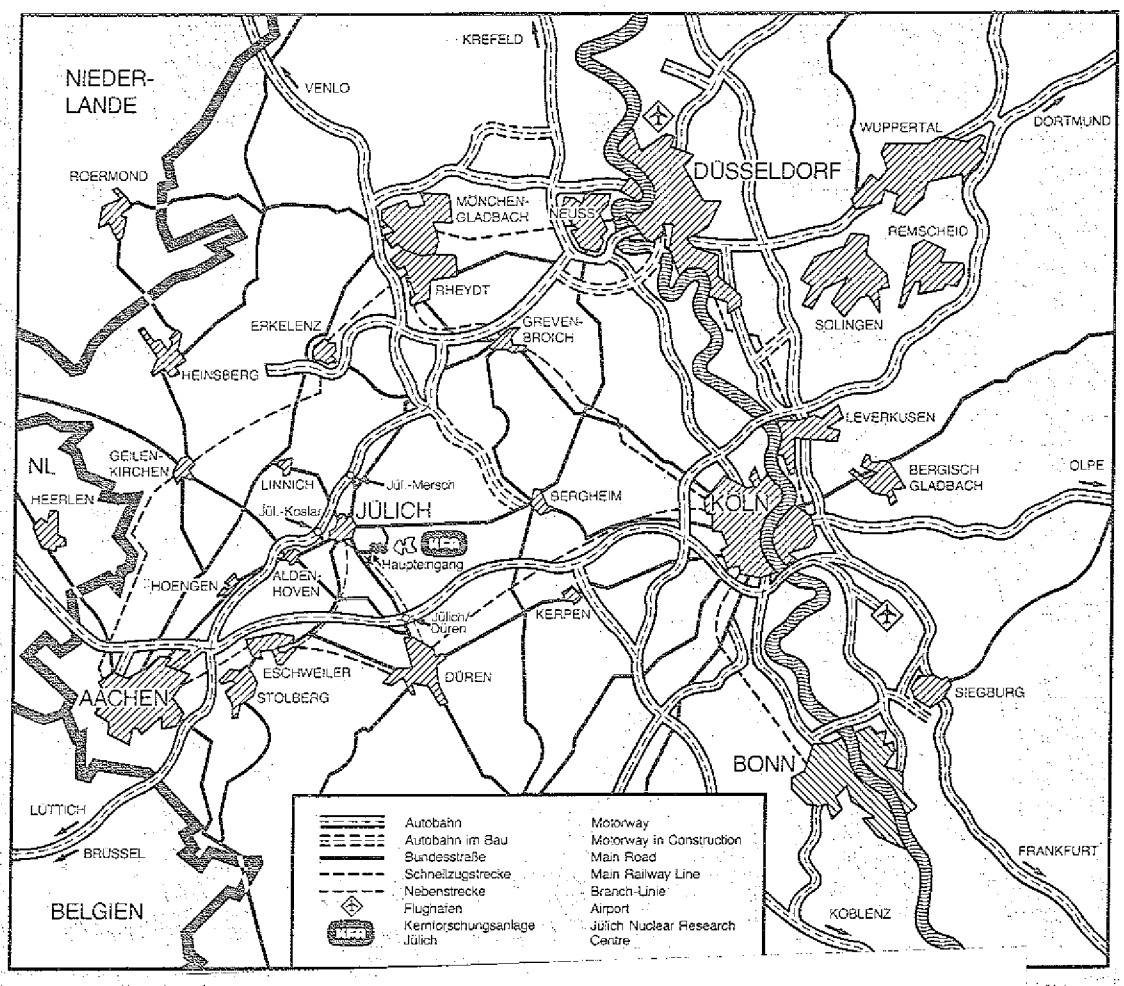

Als Manuskript gedruckt

Spezielle Berichte der Kernforschungsanlage Jülich – Nr. 379
Institut für Reaktorwerkstoffe Jül-Spez-379

Zu beziehen durch: ZENTRALBIBLIOTHEK der Kernforschungsanlage Jülich GmbH
Postfach 1913 · D-5170 Jülich (Bundesrepublik Deutschland)
Telefon: 02461/610 · Telex: 833556-0 kf d

PLASTICITY
– A LIMITING CASE OF CREEP

by

H. Cords, G. Kleist, R. Zimmermann

Zeitunabhängige Plastizität als Grenzfall des Kriechens

von

H. Cords
G. Kleist
R. Zimmermann

Kurzfassung

Die vorliegende Arbeit ist ein Versuch zur Fortführung der vereinheitlichenden theoretischen Beschreibung der Stoffgleichungen für zeitunabhängige und zeitabhängige plastische Effekte in metallischen Werkstoffen. In vergleichbaren Untersuchungen werden üblicherweise zeitunabhängige plastische Dehnungen und die Dehnungen aus Kriechverformungen aus einer gemeinsamen Spannungs/Dehnungs-Beziehung unter Verwendung einer inneren Rückspannung als nicht-elastische Dehnraten ermittelt. Einige neuartige Konzepte, die die Definition der inneren Spannung, das plastische Fließen und die Materialverfestigung betreffen, werden vorgestellt, mathematisch formuliert und im Vergleich mit einer qualitativen Standardform eines Materialverhaltens getestet.

Als Ergebnis der Untersuchungen wird ein System simultaner Differentialgleichungen definiert, das es gestattet, eine Reihe von unterschiedlichen Materialeigenschaften unter einem gemeinsamen Aspekt zusammenzufassen, so z.B. normales und inverses Primärkriechen, rückgewinnbare Kriechdehnung, Inkubationszeit und Anelastizität in Spannungsreduktionsversuchen, negative Spannungsrelaxation, plastisches Fließen, ideale Plastizität, abfallende Fließspannung trotz erhöhter Dehnrate, Portevin - Le Chatelier Effekt, Verfestigung bei einsinniger und zyklischer Belastungsform. Der theoretische Ansatz begründet sich hauptsächlich auf eine Querdehnungsbewegung der Materialprobe, die nicht wie sonst üblich der longitudinalen Dehnungsbewegung durch Vorgabe eines konstanten Querkontraktionskoeffizienten steif folgt, sondern die als Bewegung verstanden wird, die der Axialbewegung mit zeitlicher Verzögerung nachschleift und gleichzeitig eine Behinderung darstellt.

Plasticity - A Limiting Case of Creep

Kernforschungs-anlage Jülich GmbH IRW	JÜL-Spez-379	November 1986

Plasticity - A Limiting Case of Creep

by

H. Cords
G. Kleist
R. Zimmermann

Abstract

The present work is an attempt to develop further the so-called unified theory for viscoplastic constitutive equations as used for metals or metal alloys. Typically, in similar approaches creep strains and plastic strains are derived from one common stress-strain relationship for inelastic strain rates employing an internal stress function as a back stress. Some novel concepts concerning the definition of the internal stress, plastic yielding and material hardening have been introduced, formulated mathematically and tested for correspondence with a standard type of materials behaviour.

As a result of the investigations a system of simultaneous differential equations is defined which has been used to elaborate a common view on a number of different material effects observed in creep and plasticity i.e. normal and inverted primary creep, recoverable creep, incubation time and anelasticity in stress reduction, negative stress relaxation, plastic yielding, perfect plasticity, negative strain rate sensitivity, serrated flow, strain hardening in monotonic and cyclic loading. The theoretical approach is mainly based on a lateral contraction movement not following rigidly the longitudinal extension of the material specimen by a prescribed constant value of Poisson's ratio as usual, but following the axial extension in a process of drag which allows for retardation and which simultaneously impedes the longitudinal straining.

Table of Contents

1.0 Introduction

Traditionally creep is considered as a time-dependent deformation process while deformations due to plasticity occur so rapidly that a specific time dependence is usually not accounted for. The theory of viscoplasticity, however, represents a unifying approach on the basis of a time dependence for both phenomena. Viscoplasticity is a convenient method for numerical stress-strain analyses as employed for complex components.[1] Time-independent plasticity relies upon a flow rule which allows plastic deformation to occur only if a yield surface in a stress space σ is reached, i.e. speaking in uniaxial terms, plastic deformation occurs if the excess stress $\sigma - \sigma_p$ is not negative where σ_p is a yield point stress. In a similar fashion, in the more recent development of creep laws it was found highly advantageous not to refer simply to a stress σ but rather to refer to a stress difference $\sigma - \sigma_i$ where σ_i is an internal stress function.[2] Both flow rule and creep law can be commonly defined on the basis of an excess stress insinuating that a relationship between $\sigma - \sigma_p$ and $\sigma - \sigma_i$ exists. Therefore a part of the present investigation is dedicated to developing an understanding of the internal stress function σ_i which can shed some light on a possible relationship between yield point stress σ_p and internal stress σ_i. The physical meaning of the internal stress function σ_i has been extensively discussed (see e.g. references[3],[4]). In most cases the internal stress is vaguely attributed to long-distance interactions between grains or precipitates or to interactions between dislocation lines. The given definitions are founded on microscopic properties of the material although the internal stress also strongly affects the macroscopic properties of a creeping specimen. It is the intention to provide a definition of the internal stress σ_i entirely based on its macroscopically observable effects. Thus mathematical relationships involving the internal stress can become integrated parts of the theory of continuum mechanics, and can serve as constitutive equations.

To explain the concept further it is useful to discuss an idea described by Booij.[5] According to his understanding the material is heterogeneous consisting of two portions, the one part being elastic, the other part being inelastic. The model applies to both creep and plasticity. In a uniaxially loaded specimen internal lateral stresses $\sigma_{i_{rr}}$ exist as a consequence of mechanical interaction between the two parts of the material :

- That part of the material which responds elastically tends to acquire a lateral contraction given by a Poisson's ratio $\nu < 1/2$. The remaining part of the material which responds inelastically tends to attain a lateral contraction given by a Poisson's ratio $\nu = 1/2$. The two portions, intimately mixed together and subjected to the compatibility condition of continuum mechanics, cannot produce individual lateral contractions but instead they produce an internal mechanical stress $\sigma_{i_{rr}}$ in the radial direction of the specimen, and are forced to have a common lateral contraction corresponding to the physically measured value of Poisson's ratio ν.

This situation exists immediately upon loading. Subsequently it would seem natural to assume that the internal radial stress $\sigma_{i_{rr}}$ has the ability to relax. Under such circumstances relaxation can be envisaged if during the course of time the two parts of the material agree upon a common value of

---

1 D.R.J.Owen, E.Hinton - Finite Elements in Plasticity, Theory and Practice , Pineridge Press Ltd, 1980, p.95

2 E.Krempl, J.J.McMahon, D.Yao - Viscoplasticity Based on Overstress with a Differential Growth Law for the Equilibrium Stress, NASA Symposium, Cleveland, Ohio, June 13-15, 1984

3 J.L.Chaboche - On the Constitutive Equations of Materials under Monotonic or Cyclic Loadings, Rech. Aerosp. 1983-85

4 B.Ilschner - Hochtemperatur-Plastizität , Warmfestigkeit und Warmverformbarkeit metallischer Werkstoffe, Springer-Verlag Heidelberg, 1973, S.275

5 J.Booij - Computer Program for Testing Constitutive Relations in Creep and Plasticity, Department of Mechanical Engineering, Delft University of Technology, The Netherlands, WTHD Nr.104, Report Nr.618, Dec 1977

Poisson's ratio. Considering an incompressible material the common value is necessarily $\nu = 1/2$. The small, intermediate changes in volume due to internal elastic straining are usually disregarded in applications with creep or plastic flow.[6] It is important to point out that the internal stress $\sigma_{i_{rr}}$ as presently introduced is in direct correspondence with the small volume changes which occur as a result of simultaneous elastic and plastic deformations. Therefore, the condition of incompressibility is strictly speaking only applicable if the two equal volumes obtained before und after plastic deformation both refer to a specimen which is free of stress. Neglecting small changes in volume due to elastic straining is equivalent to the neglect of the macroscopic effects caused by the internal stress $\sigma_{i_{rr}}$. The statement can be rephrased positively :

- In addition to the axial stress-strain relationship there inherently exists a radial stress-strain relationship correlating the internal radial stress $\sigma_{i_{rr}}$ with a corresponding amount of physically measureable radial strain ε_{rr}.

The radial strain can be observed in an uniaxial creep experiment followed by a strain-hold experiment to enable the relaxation of stresses. It is useful to discuss this experiment in some detail because the described procedure is subsequently employed as a guideline for the development of a mathematical description.

Upon loading, the cylindrical specimen shows an immediate lateral contraction determined by Poisson's ratio ν . During the creep test performed at constant stress there is further lateral contraction in order to meet the condition of no change in volume (incompressibility). Finally, there is lateral contraction during the subsequent strain-hold experiment. During this phase the lateral movement of the cylindrical surface is obviously retarded if compared with the axial straining because the internal flow of the material is constrained by friction as described above. It is understood that after a long time when the specimen is totally stress relaxed and when the specimen reverts to its initial volume all lateral contraction movement will stop. Currently, stress relaxation is mostly described by reversed axial creep alone. The above description allows the conjecture that the method has to be complemented to include the special properties of the internal friction forces. In the present approach the lateral contraction movement during a stress relaxation experiment is considered to be a direct response to the relaxation of the internal radial stress component $\sigma_{i_{rr}}$. Therefore an independently formulated stress relaxation law is required.

In order to promote the conceptual understanding it was found useful to replace the internal radial stress $\sigma_{i_{rr}}$ by an externally applied equivalent stress σ_{rr}. Naturally the internal stress $\sigma_{i_{rr}}$ is expected to be distributed somehow within the cylindrical specimen. However, for mechanical applications the details of a distribution function for $\sigma_{i_{rr}}$ are not required the same way as the distribution function of the internal counterpart of an axially applied, external stress is not required as long as the test specimen is considered to be a small sample of material. The equivalent stress σ_{rr} is introduced as a substitute for the internal stress distribution $\sigma_{i_{rr}}$ with opposite sign. It is a constant stress distribution radially applied to the cylindrical surface of the specimen. Its value is determined so as to sustain the same radial strain ε_{rr} as the one sustained by the internal stress $\sigma_{i_{rr}}$. Experimentally an equivalent external stress can be conceived of as being a radially applied stress quasi-statically compensating for the lateral contraction movement caused by the slow collapse of the internal radial stress $\sigma_{i_{rr}}$ during relaxation.

In reversing cause and effect a radial contraction constraint $\hat{\varepsilon}_{rr}$ can cause an external stress equivalent to the internal radial stress $\sigma_{i_{rr}}$ at any time. Furthermore in a tensile creep experiment the equivalent radial stress which is obviously tensile also causes lateral contraction in the axial direction. As in an initial action there is a tensile stress σ applied in the axial direction, the additional axial contraction caused by a radial contraction constraint results in an internal back stress $\sigma_{i_{zz}} = \sigma_i$. Therefore the effective stress for creep is a superposition of both stresses, $\sigma + \sigma_i$, where σ_i is negative for a tensile axial stress σ .

In the present work the effective stress $\sigma + \sigma_i$ is used in a conventional power law for steady-state creep as proposed by Norton.[7] The special properties of the radial contraction constraint $\hat{\varepsilon}_{rr}$ are postulated by means of an independently formulated relaxation law. The creep law and the relaxation law constitute a system of differential equations to be solved simultaneously as an initial value problem. The functional properties of the mathematical formulation are then studied by means of numerical evaluations with relevance to various creep experiments. The results are found to be in qualitative agreement with a standard type of materials behaviour. The procedure followed is characteristic for the first stage in the development of a creep law when it is important to clarify whether

---

6 A.M.Freudenthal and H.Geiringer, The inelastic continuum, Encyclopedia of Physics, edited by S.Flügge, Vol VI, Elasticity and Plasticity, Springer Verlag, Berlin 1958, p. 279

7 F.Norton - Creep of Steel at High Temperatures, p. 67 Mc Graw-Hill, New York , 1929

certain experimental effects are included in the mathematical formulation or not. At this stage no attempt was made to obtain quantitative agreement with experimentally measured creep curves. The numerical analyses concerning creep are described in the first part of the paper. The results were encourageing enough to extend the development towards higher stresses and higher loading rates in the sense of a unified theory for visco-plasticity. The additional properties of the extended formulation are discussed in the second part of the paper.

2.0 Elastic Calculations Including Lateral Contraction Constraints

The definition of the internal stress σ_i as outlined conceptually in the introduction will be given a more mathematical basis. The special nature of the internal stress σ_i as related to an externally applied stress σ will also be elaborated in greater detail.

The elastic stress-strain relationship including lateral contraction is represented by the following matrix relationship

$$\begin{pmatrix} \varepsilon_{rr} \\ \varepsilon_{\theta\theta} \\ \varepsilon_{zz} \end{pmatrix} = \frac{1}{E} \begin{pmatrix} 1 & -\nu & -\nu \\ -\nu & 1 & -\nu \\ -\nu & -\nu & 1 \end{pmatrix} \begin{pmatrix} \sigma_{rr} \\ \sigma_{\theta\theta} \\ \sigma_{zz} \end{pmatrix} \tag{1}$$

with

E	modulus of elasticity
ν	Poisson's ratio
ε	strain
σ	stress.

The coordinates r (radial), θ (azimuthal) and z (axial) refer to a coordinate system located at the symmetry centre of a cylindrical test specimen. The loading conditions are such that shear strains and shear stresses need not be considered. The inverse of equation (1) is

$$\begin{pmatrix} \sigma_{rr} \\ \sigma_{\theta\theta} \\ \sigma_{zz} \end{pmatrix} = \frac{E}{(1+\nu)(1-2\nu)} \begin{pmatrix} 1-\nu & \nu & \nu \\ \nu & 1-\nu & \nu \\ \nu & \nu & 1-\nu \end{pmatrix} \begin{pmatrix} \varepsilon_{rr} \\ \varepsilon_{\theta\theta} \\ \varepsilon_{zz} \end{pmatrix}. \tag{2}$$

- In a first consideration a tensile experiment is conceived of during which lateral contraction is fully constrained, i.e. $\varepsilon_{rr} = \varepsilon_{\theta\theta} = 0$. The load applied in the axial direction is $\sigma_{zz} \neq 0$. Due to this simplification the third of the set of equations (2) can be easily reversed again, i.e.

$$\varepsilon_{zz} = \frac{1}{E} \frac{(1+\nu)(1-2\nu)}{(1-\nu)} \sigma_{zz} \tag{3}$$

and compared with the third of the set of equations (1),

$$\varepsilon_{zz} = \frac{1}{E} (\sigma_{zz} - \nu\sigma_{rr} - \nu\sigma_{\theta\theta}) \tag{4}$$

which represents the same relationship as equation (3) in a different form.

- However, a similar experiment (second consideration) with no lateral contraction constraint would result in

$$\varepsilon_{zz} = \frac{1}{E} \sigma_{zz} \tag{5}$$

because in such a case there will be no radial and azimuthal stresses, $\sigma_{rr} = \sigma_{\theta\theta} = 0$. Equation (5) can be derived from the third of the set of equations (1). A comparison of the two experiments, i.e. a comparison between the two equations (4) & (5), shows that the axial stress

$$\sigma_i = -\nu\sigma_{rr} - \nu\,\sigma_{\theta\theta} \tag{6}$$

is entirely due to the lateral contraction constraint.

- The third experiment to be considered is the one where the axial direction is fully constrained $\varepsilon_{zz} = 0$ and a radial strain $\hat{\varepsilon}_{rr}$ is applied. For reasons of symmetry there will be also an azimuthal strain $\hat{\varepsilon}_{\theta\theta} = \hat{\varepsilon}_{rr}$. Under such conditions the first two of the set of equations (2) provide the relationship:

$$\sigma_{rr} = \frac{E\,\hat{\varepsilon}_{rr}}{(1+\nu)(1-2\nu)} \tag{7}$$

and

$$\sigma_{\theta\theta} = \frac{E\,\hat{\varepsilon}_{rr}}{(1+\nu)(1-2\nu)}. \tag{8}$$

The three experiments are related to each other by the following additional requirements:

Firstly, the amount of radial strain $\hat{\varepsilon}_{rr}$ applied in the third experiment is chosen to be the same as that one which is constrained in the first experiment. A variable amount of applied radial strain $\hat{\varepsilon}_{rr}$ corresponds to a variable amount of constrained lateral contraction in the first experiment.

Secondly, the geometries of the loaded specimens used in the second and third experiment are chosen to be identical, such that a superposition of the two stress-strain situations is possible.

Thus, introducing σ_{rr} and $\sigma_{\theta\theta}$ from equations (7) & (8) into equation (6) yields an axial back stress

$$\sigma_i = \frac{-2\nu E}{(1+\nu)(1-2\nu)}\,\hat{\varepsilon}_{rr}. \tag{9}$$

Equation (9) provides the axial stress component σ_i from a specifically chosen amount of constrained lateral contraction expressed as a value of strain, i.e. $\hat{\varepsilon}_{rr}$.

It is of some interest to discuss the above equations with special reference to the concept explained in the introduction. Usually in a uniaxial elastic experiment a lateral contraction constraint is not considered. The axial stress-strain relationship is Hooke's law, i.e. equation (5), complemented by the specification of a lateral strain $\varepsilon_{rr} = -\nu\sigma_{zz}/E$. According to the outlined concept a lateral contraction constraint is being introduced as an additional measure to prevent the specimen from having a spontaneous lateral contraction $\varepsilon_{rr} = -1/2 \quad \sigma_{zz}/E$. This is to prevent the specimen from going spontaneously plastic ($\nu = 1/2$) on application of any small load σ_{zz}. The internal radial stress $\sigma_{i_{rr}}$ is considered to be the cause of the material not going plastic at a small value of axial load.

There are obviously two equivalent possibilities to characterize the onset of plasticity i.e. either Poisson's ratio assumes the value one half, or the internal stress $\sigma_{i_{rr}}$ collapses with a subsequent release of the corresponding lateral contraction expressed as a value of radial strain

$$\varepsilon_{rr} = \frac{-(\frac{1}{2} - \nu)\ \sigma_{zz}}{E}. \tag{10}$$

For all subsequent applications we have chosen the controlling of the quantity $\varepsilon_{rr} = -\hat{\varepsilon}_{rr}$ for the onset of plasticity. Therefore the Poisson's ratio ν remains a characteristic constant for lateral contraction during elastic straining. For abbreviation all subscripts zz are omitted from the formulation. The elastic stress-strain relationship derived from equations (4) & (6) including lateral contraction constraints is

$$\varepsilon^{el} = \frac{\sigma + \sigma_i}{E}. \tag{11}$$

For subsequent use under elasto-plastic conditions additional symbols are introduced. The elastic stress σ and the Young's modulus E will be labelled $\bar{\sigma}$ and $\bar{E}$ with identical meaning in the elastic regime. Equation (11) is then replaced by

$$\dot{\varepsilon}^{el} = \frac{\dot{\bar{\sigma}} + \dot{\sigma}_i}{\bar{E}}. \tag{12}$$

According to equations (11) & (12) the elastic strain ε^{el} consists of two parts one of which, i.e. $\varepsilon_1^{el} = \bar{\sigma}/\bar{E}$, is truly elastic. The second contribution of elastic strain $\varepsilon_2^{el} = \sigma_i/\bar{E}$ is elastically speaking not existent for low values of stress but is further discussed when plastic effects are included (sections 3 & 6). Also, the idea of a lateral contraction constraint $\hat{\varepsilon}_{rr}$ defined entirely for static conditions in the present section is further developed in section 4 to provide a dynamic quantity $\hat{\varepsilon}_{rr}$ for the conditions of creep and plasticity.

3.0 Introduction of a Creep Law

Classically creep is introduced as a time dependent phenomenon. In analogy to Hooke's law for elastic deformation, equation (5), obviously the simplest approach to the problem would be to propose a linear relationship between stress $\bar{\sigma}$ and strain measured per unit of time $\dot{\varepsilon}^c$

$$\dot{\varepsilon}^c = \frac{1}{K}\ \bar{\sigma}. \tag{13}$$

Equation (13) characterizes creep as used in the theory of linear visco-elasticity.

In the present paper the general assumption is that all axial stresses $\bar{\sigma}$ are influenced by the effect of a lateral contraction constraint. Yielding to this demand the creep law, equation (13), has to be modified and an additional axial stress σ_i has to be added to the externally applied stress $\bar{\sigma}$ in order to have an effective creep stress $\bar{\sigma} + \sigma_i$. Accordingly, equation (13) has to be rewritten as

$$\dot{\varepsilon}^c = \frac{1}{K}\ (\bar{\sigma} + \sigma_i). \tag{14}$$

The stress $\bar{\sigma} + \sigma_i$ discussed in the previous section is considered to be the driving force for creep.

In the present analysis we are mostly interested in the creep at stresses where the so-called power law creep which is based on dislocation movements is dominating. Under such circumstances the creep law will not be that of equation (14) but rather a highly non-linear relationship such as

$$\dot{\varepsilon}^c = \text{sign}\ (\bar{\sigma} + \sigma_i)\ \left|\frac{\bar{\sigma} + \sigma_i}{K}\right|^n. \tag{15}$$

The constant K is called the drag stress while the exponent n is the creep exponent or the Norton exponent n. If the drag stress K is surmounted by the effective stress $\bar{\sigma} + \sigma_i$ then the creep rate $\dot{\varepsilon}^c$ will be greatly increased.

4.0 Introduction of a Relaxation Law

In order to derive a mathematical formula for the purpose of a quantitative description of stress relaxation the creep experiment described in the introduction is reconsidered.

It is assumed that at the start of the creep experiment, the cylindrical test specimen has a radius r_0 and thereafter, due to a continuous deformation the radius is a function of time $r = r(t)$. The same specimen carrying the tensile load $\bar{\sigma}$ in axial direction has a reduced radius $r\,(1 - \nu\bar{\sigma}/E)$.

Further it is assumed that during the creep experiment at any instant of time t the specimen has accumulated a creep strain ε^c, i.e. a total strain of

$$\varepsilon = \bar{\sigma}/E + \varepsilon^c \tag{16}$$

has been reached.

There is a third radius necessary to determine the radial contraction constraint $\hat{\varepsilon}_{rr}$ (section 2) under the conditions of a simultaneously proceeding creep deformation. It is the radius $r_0 e^{-1/2\,\varepsilon}$ obtained by the assumption that the same total strain ε was obtained for an incompressible material. It is the same radius which can be obtained realistically by interrupting the creep experiment at any instant of time t for a stress relaxation experiment with the strain hold condition $\dot{\varepsilon} = 0$ applied. At the point in time when the relaxation experiment starts depending on the current value of r there is a difference Δr expected to exist between the two radii i.e. the current one under load and the one ultimately reached by stress relaxation.

$$\Delta r = r(1 - \nu\frac{\bar{\sigma}}{E}) - r_0 e^{-1/2\ (\bar{\sigma}/E + \varepsilon^c)} \tag{17}$$

At the end of the relaxation experiment ($t = \infty$) when the specimen is free of stress ($\bar{\sigma} = 0$ and $\sigma_i = 0$), there will be no radial displacement ($\Delta r = 0$) , and then it follows from equation (17) that

$$r = r_0\, e^{-1/2\ \varepsilon^c}. \tag{18}$$

Equation (18) is expected to be valid for an elongation of the cylindrical specimen with no change in volume.

The radial displacement Δr corresponds to a radial strain $\hat{\varepsilon}_{rr} = \Delta r/r$. That is:

$$\hat{\varepsilon}_{rr} = (1 - \nu\frac{\bar{\sigma}}{E}) - \frac{r_0}{r}\, e^{-1/2\ (\bar{\sigma}/E + \varepsilon^c)}. \tag{19}$$

By substituting $\hat{\varepsilon}_{rr}$ in equation (9) the internal stress σ_i is defined in terms of the constrained lateral contraction Δr. Equation (17) can be evaluated from the given set of formulae provided that the function $r = r(t)$ is known.

In order to define the radial contraction as a function of time it is tentatively assumed that radial contraction occurs at a rate proportional to the momentarily existing amount of constrained lateral contraction Δr, i.e.

$$\dot{r} = -\tilde{\kappa}\Delta r \tag{20}$$

with a constant value for $\tilde{\kappa}$.

The simple assumption represented by equation (20) has to be improved slightly in order to fulfil some obvious experimental requirements. To show the necessity of such an action Δr from equation (17) is introduced into equation (20):

$$\dot{r} + \tilde{\kappa}(1 - \nu\frac{\bar{\sigma}}{E})r = \tilde{\kappa} r_0\, e^{-1/2\ (\bar{\sigma}/E + \varepsilon^c)}. \tag{21}$$

Equation (21) is a linear differential equation of first order, well known from several other physical applications. The term on the right hand side plays the rôle of a generator term :

- If the value on the right hand side of equation (21) is lowered by application of some stress $\bar{\sigma}$ and subsequent creep strain ε^c then in order to keep equality the left hand side of equation (21) is also to be lowered in value. Lower values on the left hand side are promptly obtained by lower values for $\dot{r}$. At the start of the creep experiment the rate of change in radius will promptly turn negative ($\dot{r} < 0$) to produce a lower r during the course of time. With a lower value for r after some time the second term on the left hand side of equation (21) has balanced the action of raising $\bar{\sigma}$ while the radial rate of change $\dot{r}$ returns to normal. Thus the generator term has generated a new r.

The time $\tilde{\tau}$ necessary to complete the whole process is known to be related to the coefficient of r in equation (21), i.e.

$$\tilde{\tau} = \left[\tilde{\kappa}(1 - \nu\frac{\bar{\sigma}}{E})\right]^{-1}. \tag{22}$$

The announced requirements to meet experimental findings are the following :

- Firstly, the relaxation time τ must be the same, irrespective of the applied stress $\bar{\sigma}$ being tensile or compressive. The requirement is not met by $\tilde{\tau}$ from equation (22).
- Secondly, for a plastic flow behaviour the generator term in equation (21) must not be allowed to cause extremely high values of $\dot{r}$. A high value of $\dot{r}$ is related with an unrealistically high internal stress σ_i via the equations (20), (17), (19) & (9).

In the latter case the radial contraction movement necessary to relax the internal stress is greatly retarded. The specimen coming under tensile load experiences an initial large volume dilatation with a correspondingly large value of internal stress. It is likely that by a quick load application the material fails in a brittle manner. In order to control the plastic flow behaviour of the material, i.e. to avoid brittle failure conditions, the relaxation time $\tilde{\tau}$ has to be coupled to the axial strain rate $\dot{\varepsilon}^c$.

Having such improvements in mind the constant $\tilde{\kappa}$ of equation (20) is to be replaced by means of equation (23)

$$\tilde{\kappa} = \frac{\kappa + \lambda\,|\dot{\varepsilon}^c|}{1 - \nu\frac{\bar{\sigma}}{E}} \tag{23}$$

and equation (21) transforms into

$$\dot{r} + (\kappa + \lambda\,|\dot{\varepsilon}^c|)r = \frac{\kappa + \lambda\,|\dot{\varepsilon}^c|}{1 - \nu\frac{\bar{\sigma}}{E}}\, r_0\, e^{-1/2\ (\bar{\sigma}/E + \varepsilon^c)}. \tag{24}$$

The relaxation time incorporated in equation (24) is independent of the direction of load. The second requirement is also met and this can be shown by the asymptotic behaviour of the generator term of equation (24) for very high axial strain rates $\dot{\varepsilon}^c$.

$$\dot{r}_g \cong \operatorname{sign}(\dot{\varepsilon}^c)\,\frac{2\lambda}{t}\, r_0 \left[1 - (\frac{1}{2} - \nu)\,\frac{\bar{\sigma}}{E}\right] \tag{25}$$

In the approximation, equation (25), in which $\varepsilon^c = \dot{\varepsilon}^c t$ was used, the rate of radial contraction $\dot{r}_g$ is inversely proportional to the time and directly proportional to the constant λ which is a measure of the ductility of the material. The term in square brackets shows that the generator term operates with a complementary Poisson's ratio $(1/2 - \nu)$ where ν is the elastic value of Poisson's ratio. The constant κ also involved in the relaxation law is the inverse of the relaxation time typical for the low stress situation where the axial strain rate $\dot{\varepsilon}^c$ is low.

5.0 Numerical Evaluations Using the Combined Creep/Relaxation Law

5.1 Constant Stress Creep Experiments

The four constants incorporated into the creep/relaxation law were given arbitrary values (see Table I)

Table I : Values chosen for the numerical studies concerning creep	
drag stress	K = 133,7 MPa
Norton exponent	n = 6.71
relaxation coefficient	κ = 0.0432 h^{-1}
ductility coefficient	λ = 494.8
Young's modulus	E = 118 797 MPa
Poisson's ratio	ν = 0.3

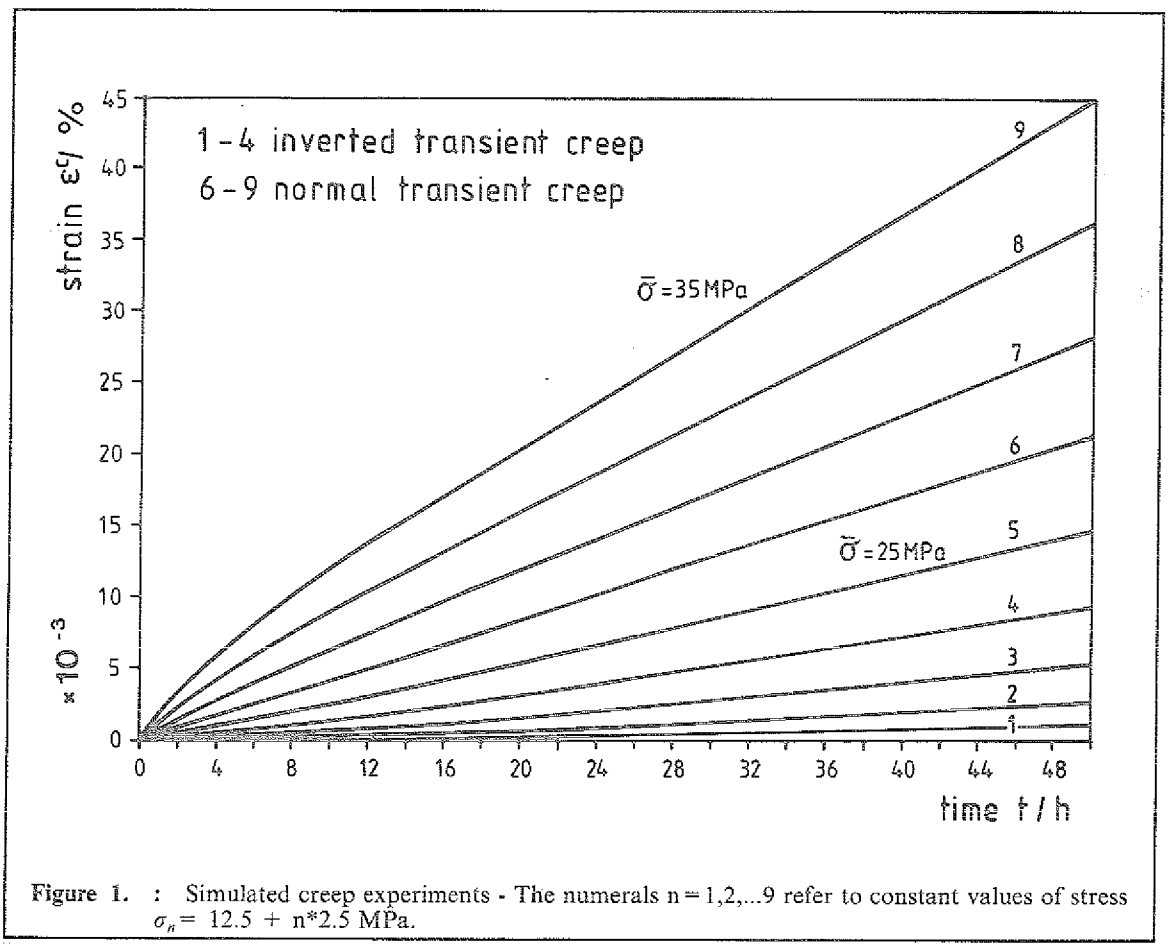

Figure 1. : Simulated creep experiments - The numerals n = 1,2,...9 refer to constant values of stress σ_n = 12.5 + n*2.5 MPa.

To simulate a constant stress creep experiment, the stress $\bar{\sigma}$ was rapidly raised to its nominal value and subsequently kept constant. The results from calculations for a number of nominal stress values are shown in Figure 1. Creep curves obtained at lower values of stress, $\bar{\sigma} < 25$ MPa show the phe-

nomenon of inverted transient creep while all other curves with $\bar{\sigma} > 25$ MPa show a normal primary creep behaviour. An explanation can be given in terms of the concept presented here:

- Upon loading there is a lateral contraction constraint characterized by a lateral strain, $-(1/2 - \nu)\,\varepsilon^{el}$. Subsequent creep causes further lateral contraction, $-1/2\,\varepsilon^{c}$. However, contrary to the elastic case, the lateral contraction due to creep strains ε^c does not occur instantaneously. Therefore, in the present analysis it is recorded as a target value which is ultimately reached. It is instantaneously recorded as enhancing the existing amount of lateral contraction constraint. According to equation (9) the amount of lateral contraction constraint $\hat{\varepsilon}_{rr}$ is proportional to the internal stress σ_i. Thus creep primarily causes an internal stress σ_i which tends to resist the movement of creep deformation. The internal back stress σ_i is raised at a rate which depends on the creep rate, $\dot{\varepsilon}^c$. Simultaneously the internal back stress σ_i can relax at a rate $\dot{\sigma}_i$. The two processes which work in opposite directions balance each other after some time to cause a stationary creep rate which is restrained by a constant value of internal back stress σ_i. Inverted transient creep occurs if the absolute value of σ_i obtained by the initial rapid loading is greater than the equilibrium value for σ_i. In this case creep is initially restrained by a greater value in back stress σ_i. Conversely, normal primary creep occurs if the initial absolute value of σ_i is smaller than the equilibrium value for σ_i. A more complete description of the mechanisms involved is given in the subsequent Section 5.2.

5.2 Creep Experiments with Step Loading

Experimental results of creep with two interchanging levels of constant tensile load are reported for instance by Ilschner.[8] The peculiarity of such experiments is that upon each change in load the creep strain rate is unbalanced. The feature is best represented in a plot $\ln\dot{\varepsilon}^c$ versus ε^c. The experiments show an inverted transient creep behaviour upon each change in stress if the applied stress is generally low. A normal transient creep behaviour is displayed upon each change in load if reversed step changes in stress occur at a high level of stress. In between there is apparently a well defined limit value in stress or strain rate. More precisely expressed, the characteristic quantity $\mathrm{sign}(\Delta\bar{\sigma})\, d\dot{\varepsilon}^c/d\varepsilon^c$ observed immediately upon each step change in stress $\Delta\bar{\sigma}$ is either positive indicating inverted transient creep or negative indicating normal transient creep. In the first case the strain rate stabilizes in the same direction as defined by the preceding step change in stress $\Delta\bar{\sigma}$. In the second case the strain rate stabilizes in the reversed direction. Ilschner[8] showed that both characteristics can be combined in one constant load creep experiment when, during the reversed stepping procedure, the true stress is raised above the inherent limit value in a self-controlled fashion.

As shown in Figure 2 the numerical calculations using the described set of formulae for reversed step loading produce the same characteristics as observed in experiments.

---

8 B.Ilschner, Hochtemperatur-Plastizität, Reine und angewandte Metallkunde in Einzeldarstellungen, Bd 23, Springer Verlag Berlin, 1973, ISBN 3-540-05966-0, p.29

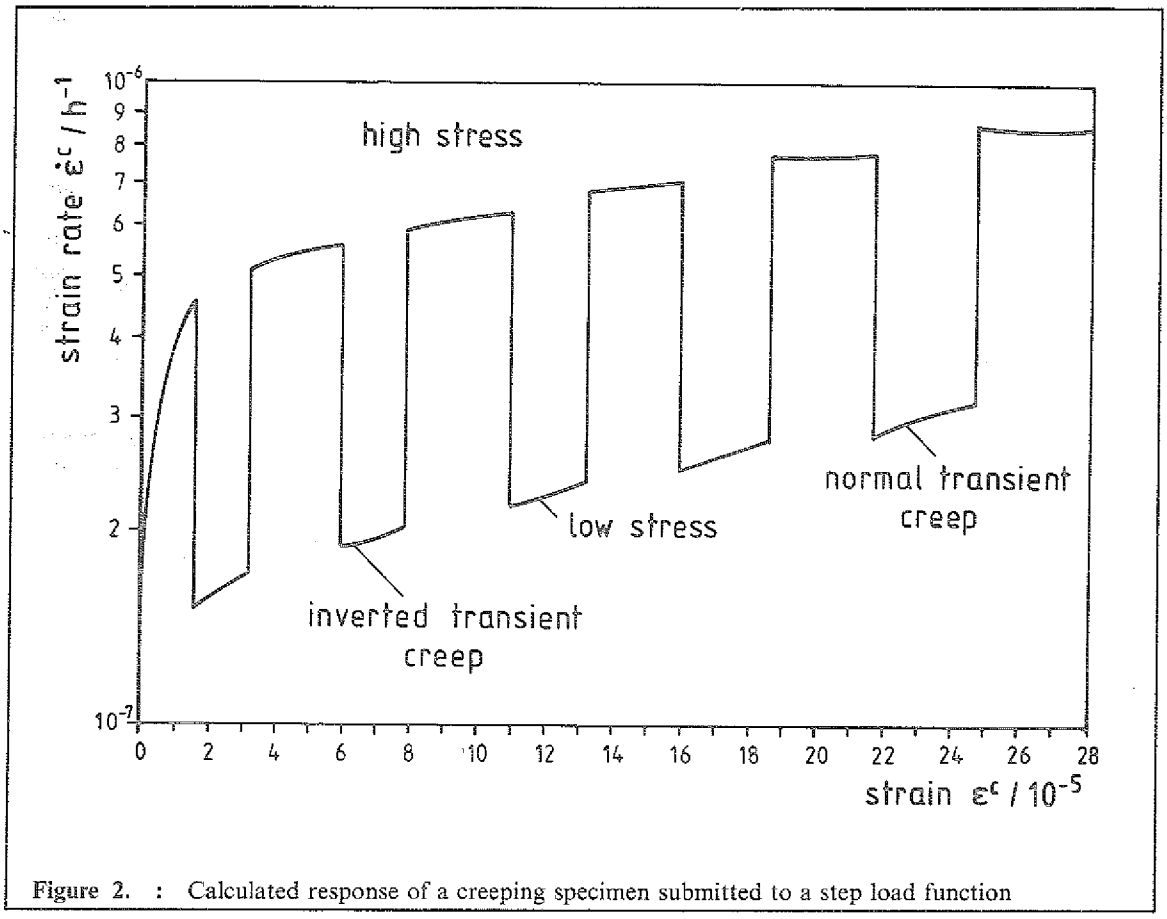

Figure 2. : Calculated response of a creeping specimen submitted to a step load function

Due to the arbitrary choice of the parameters (see Table I) the described effect was found at comparatively low levels of strain and strain rate, i.e. low as compared with the experimental results. During the calculations the stress $\bar{\sigma}$ was alternated between values of 16 and 13 MPa. In order to view both effects a continuously rising stress contribution was added, i.e. $\Delta\bar{\sigma} = 2.6{*}10^{-3}\ t$ where t is the time in hours.

The cause of the effect is a somewhat complex mechanism. Thus, prior to an explanation in terms of the present concept, four statements are given each one disclosing an interrelationsship of a qualitative kind.

- The differential ratio $d\dot{\varepsilon}^c/d\varepsilon^c$ characteristic for the transient creep behaviour can be derived from equation (15) by forming the second time derivative of the creep strain ε^c. This relationship shows that $d\dot{\varepsilon}^c/d\varepsilon^c$ is directly proportional to the rate of change in internal stress $\dot{\sigma}_i$ if after a step change the applied stress is kept constant, $\bar{\sigma}$ = constant, and if only positive strain rates, $\dot{\varepsilon}^c > 0$, are considered.

- Furthermore the rate of change in internal stress $\dot{\sigma}_i$ can be derived from equations (9) & (19) by differentiation with respect to time. As a result it can be noted that a stationary state of internal stress σ_i = constant is obtained if the ratio of strain rates $-1/2\ d\dot{\varepsilon}^c/d(\ln r) = 1$, i.e. if the radial strain rate $-d(\ln r)/dt = -\dot{r}/r$ is balanced by half of the axial strain rate, $1/2\ \dot{\varepsilon}^c$ in the sense of equation (18). Subsequent to a sudden change in the applied stress $\Delta\bar{\sigma}$ the quantity $-1/2\ d\dot{\varepsilon}^c/d(\ln r)$ is usually out of balance, i.e. $\neq 1$.

- In turn the behaviour of the quantity $-1/2\ d\dot{\varepsilon}^c/d(\ln r)$ can be studied by forming the ratio of $\dot{\varepsilon}^c$ from equation (15) divided by $\dot{r}$ from equation (20). This relationship shows that the ratio of strain rates $-1/2\ d\dot{\varepsilon}^c/d(\ln r)$ is proportional to the ratio $\dot{\varepsilon}^c/(-\sigma_i)$.

- Finally it is also important to recall that a change in stress not only causes an immediate change in strain rate $\dot{\varepsilon}^c$ but also an immediate change in internal stress σ_i via equations (20), (17), (19) & (9).

An explanation of the two different types of transient creep during step loading can be given in terms of the four statements.

- The *normal transient creep* occurs at high values of stress $\bar{\sigma}$. Due to the power law for creep, equation (14), the numerator in the ratio $\dot{\varepsilon}^c/(-\sigma_i)$ plays the dominant rôle. Subsequent to an increase in stress $\Delta\bar{\sigma}$ the strain rate $\dot{\varepsilon}^c$ is increased such that the ratio $\dot{\varepsilon}^c/(-\sigma_i)$ is increased. In turn an increase in the ratio $\dot{\varepsilon}^c/(-\sigma_i)$ is equivalent to a rise in the axial strain rate above the radial strain rate, i.e. $-1/2\, d\varepsilon^c/d(\ln r) > 1$. In such a situation there is a build up of internal back stress $(-\sigma_i)$ in order to reattain a balance between elongation and lateral contraction. The increase in back stress $(-\sigma_i)$ causes a lower axial strain rate, $d\dot{\varepsilon}^c/d\varepsilon^c < 0$. This is an adjustment of the strain rate in the opposite direction to the one caused by the initial change in stress $\Delta\bar{\sigma}$, i.e. $\mathrm{sign}(\Delta\bar{\sigma})\, d\dot{\varepsilon}^c/d\varepsilon^c < 0$. With regard to a change in stress towards a lower value, $\mathrm{sign}(\Delta\bar{\sigma}) = -1$, the situation is reversed. The axial rate of straining is immediately depressed such that the radial rate of straining is momentarily faster, i.e. $-1/2\, d\varepsilon^c/d(\ln r) < 1$. This is the situation of stress relaxation. The internal back stress $(-\sigma_i)$ relaxes such that the axial creep rate increases, $d\dot{\varepsilon}^c/d\varepsilon^c > 0$. Again the characteristic quantity for normal transient creep behaviour is negative, $\mathrm{sign}(\Delta\bar{\sigma})\, d\dot{\varepsilon}^c/d\varepsilon^c < 0$.

- The *reversed transient creep* occurs at lower values of applied stress $\bar{\sigma}$ when the strong influence of the power law is not present. Then an increase in stress $\Delta\bar{\sigma}$ immediately causes an additional amount of lateral contraction constraint which is equivalent to a certain additional amount of internal back stress $(-\sigma_i)$, such that the ratio $\dot{\varepsilon}^c/(-\sigma_i)$ is decreased and therefore the ratio of strain rates is depressed, $-1/2\, d\varepsilon^c/d(\ln r) < 1$. With the radial strain rate being greater than the axial strain rate, the internal back stress $(-\sigma_i)$ relaxes and the axial strain rate increases further after it has already been increased directly due to the initial increase in applied stress $\bar{\sigma}$, $\mathrm{sign}(\Delta\bar{\sigma})\, d\dot{\varepsilon}^c/d\varepsilon^c > 0$. Similarly, it can be shown that a stress reduction performed at at low level of stress $\bar{\sigma}$, $\mathrm{sign}(\Delta\bar{\sigma}) = -1$, is also related to a positive value of the characteristic quantity for inverted transient creep, $\mathrm{sign}(\Delta\bar{\sigma})\, d\dot{\varepsilon}^c/d\varepsilon^c > 0$.

5.3 Stress Reduction Tests

Stress reduction tests in which during a constant stress creep experiment the applied stress is suddenly decreased to a lower level are described for instance by Osthoff et al.[9] The observations made in such an experiment are the following: a sudden decrease in strain occurs due to the

- *spontaneous release of elastic strain* which is followed by a small amount of
- *anelastic strain* recovered over some time. Then follows
- an *incubation time* during which there is apparently no further creep strain ε^c accumulated. Finally a
- *new stationary strain rate* is established.

The length of incubation time is obviously correlated to the amount of stress reduced. For large stress reductions there are large incubation times. The combined stress/relaxation law as introduced in the Sections 3 and 4 can account for the effects of incubation time and anelastic recovery of strain in the following manner:

- At high levels of stress $\bar{\sigma}$ the internal stress σ_i is mostly caused by creep (see ε^c in the generator term in equation (24)). Therefore the internal stress σ_i is not greatly affected by a sharp decrease in the stress $\bar{\sigma}$. In a rapid action it is therefore possible to reduce the stress $\bar{\sigma}$ to a level comparable or lower than the instantaneous level of the internal stress $-\sigma_i$. Subsequently, according to equation (15) the strain rate $\dot{\varepsilon}^c$ is zero or very low. The state of zero creep lasts as long as the internal stress is not relaxed. However the relaxation time of the internal stress is given by equation (24) with

$$\tau = \left(\kappa + \lambda\,|\dot{\varepsilon}^c|\right)^{-1}. \tag{26}$$

  Equation (26) shows that for the condition of zero creep rate, i.e. $\dot{\varepsilon}^c = 0$, the relaxation time, $\tau = \kappa^{-1}$, is a maximum. Consequently the state of zero creep lasts the longer the better the condition $\dot{\varepsilon}^c = 0$ is satisfied in stress reduction. For extremely large reductions in stress the

---

9 W.Osthoff, H.Schuster, P.J.Ennis and H.Nickel, Creep and Relaxation Behaviour of Inconel 617, Nuclear Technology, vol.66, 1984, pp 296-307.

internal stress σ_i is more than compensated for and therefore it causes reversed creep for a short duration of time. Reversed creep is recorded as anelastic recovery of strain.

Figure 3 shows the results of calculations obtained with the stress/relaxation law. The transition to the lower stress levels were made with a stress rate $\dot{\sigma}_0$ = -2000 MPa/h.

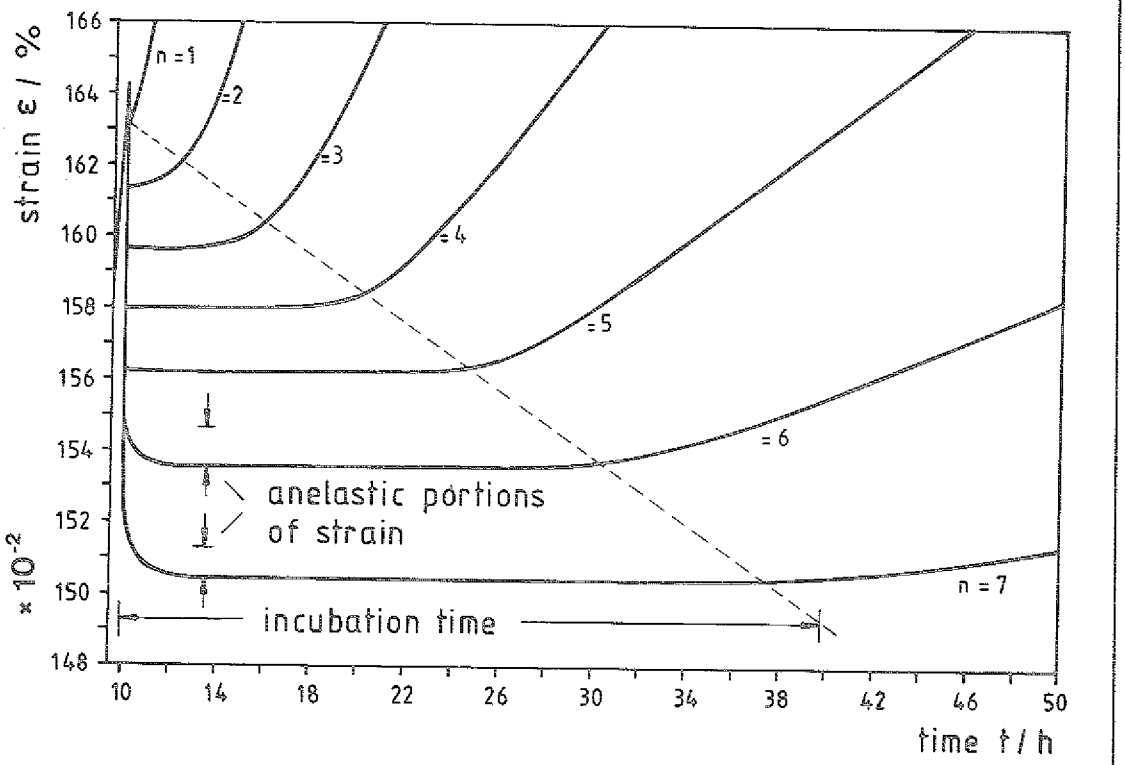

Figure 3. : Simulation of stress reduction experiments involving various levels of lower stress - After 10 hours of creep the initial value of constant stress σ_0 = 175 MPa was reduced to various lower levels of constant stresses σ_n = 180 - n*20 MPa with n = 1,2,...7. The dashed line shows how the incubation time increases with the amount of stress reduced.

5.4 *Stress Relaxation Experiments*

5.4.1 Stress Relaxation Subsequent to Creep

Stress relaxation experiments with and without the simultaneous influence of an internal stress were also studied by Osthoff et al.[10] The authors concluded that the relaxation behaviour was more satisfactorily described using the Norton creep equation modified by the internal stress σ_i than by using the conventional Norton equation, i.e.

$$\dot{\varepsilon}^c = \left(\frac{\bar{\sigma}}{K}\right)^n . \tag{27}$$

The same statement applies to the present work.

In a conventional analysis of stress relaxation the elastic strain rate $\dot{\varepsilon}^{el}$ is balanced by a reversed creep rate, $-\dot{\varepsilon}^c$. Therefore the stress relaxation rate is

[10] W.Osthoff, H.Schuster, P.J.Ennis and H.Nickel, Creep and Relaxation Behaviour of Inconel 617, Nuclear Technology, vol.66, 1984, pp 296-307.

$$\dot{\bar{\sigma}} = -E\left(\frac{\bar{\sigma}}{K}\right)^n = -\left(\frac{\bar{\sigma}}{\frac{K}{E^{1/n}}}\right)^n. \tag{28}$$

According to equation (28) the relaxation rate $\dot{\bar{\sigma}}$ becomes small if the stress $\bar{\sigma}$ is already relaxed below a certain value given by the relationship

$$\bar{\sigma} < \frac{K}{E^{1/n}}. \tag{29}$$

The drag stress K and the exponent n can be determined by means of two hot tensile tests with applied strain rates $\dot{\varepsilon}_1$ and $\dot{\varepsilon}_2$ and the corresponding stationary state stresses $\bar{\sigma}_1$ and $\bar{\sigma}_2$.

The same procedure using the same experimental values for $\dot{\varepsilon}_1$, $\dot{\varepsilon}_2$, $\bar{\sigma}_1$ and $\bar{\sigma}_2$ can be employed a second time in order to evaluate a second drag stress K and second exponent n for a creep law such as the one given by equation (15). This is particularly easy if in a simple example it is assumed that the stationary state stresses $\bar{\sigma}_1$ and $\bar{\sigma}_2$ correspond to stationary state internal stresses as follows $\sigma_{i1} = -1/2\,\bar{\sigma}_1$ and $\sigma_{i2} = -1/2\,\bar{\sigma}_2$. Due to such a simple assumption concerning the internal stress σ_i it is possible to evaluate a drag stress K which is exactly one half of the value obtained from the evaluation employing the Norton equation without internal stress. The result of such an exercise is the following statement:

- Entering the relationship (29) with values of either K or $K/2$ resulting from creep laws as given by equations (27) & (15) respectively shows that the formulation of equation (15) allows stress relaxation to a lower level in stress i.e. $\bar{\sigma} < K/(2E^{1/n})$.

Furthermore, the process of stress relaxation occurs in two stages:

- The first stage of stress relaxation is a relaxation of the stress $\bar{\sigma}$ towards the internal stress σ_i. The stress relaxation process would stop if it was not possible for σ_i to relax independently.
- Therefore, the second stage of stress relaxation is dominated by a time constant which is characteristic for the relaxation of the internal stress σ_i, i.e. that one given by equation (26).

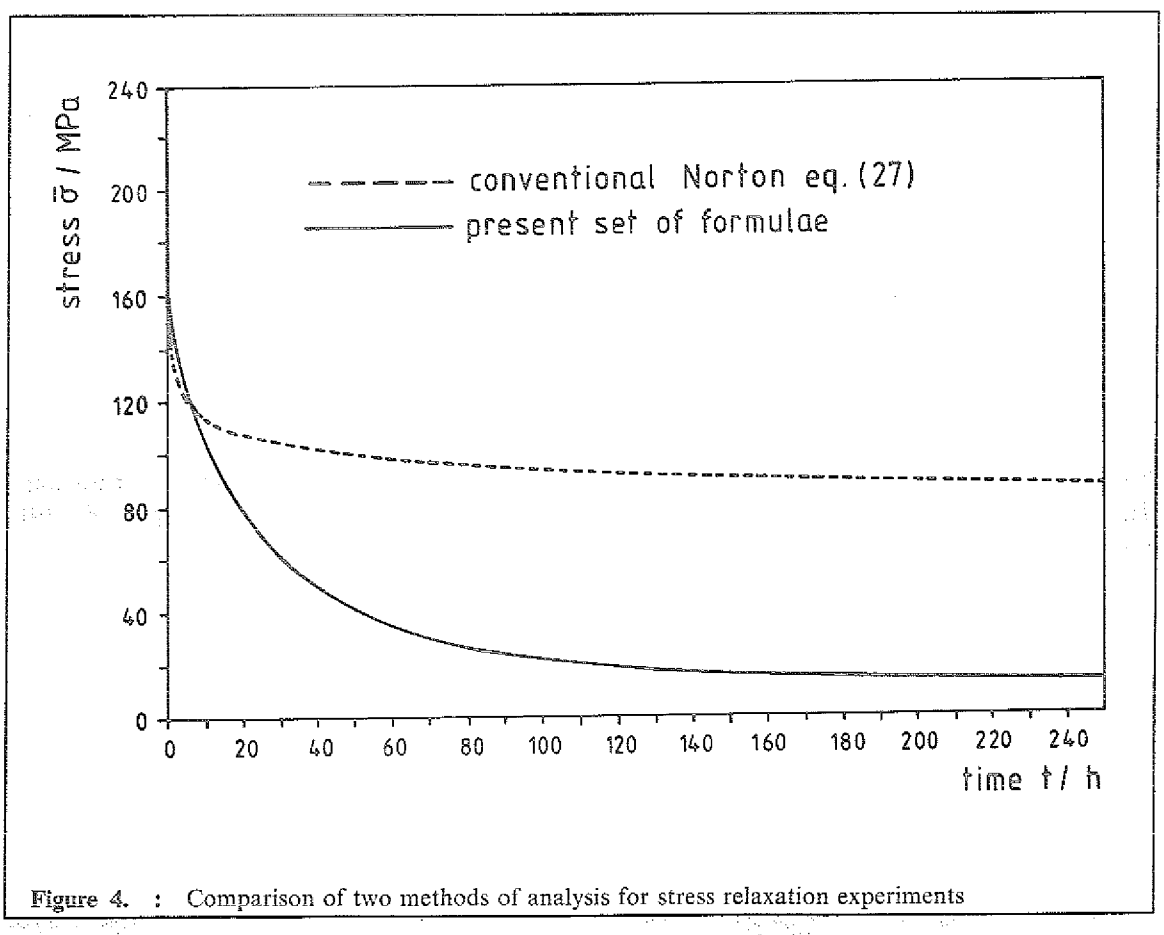

Figure 4. : Comparison of two methods of analysis for stress relaxation experiments

Two stress relaxation experiments were simulated by theoretical calculations using applied strain rates $\dot{\varepsilon}_1 = 14.4\ h^{-1}$ and $\dot{\varepsilon}_2 = 0.144\ h^{-1}$. The corresponding stationary state stresses were calculated to be $\bar{\sigma}_1 = 340$MPa and $\bar{\sigma}_2 = 240$ MPa. As described above this is sufficient information for determination of the parameters K and n of the conventional Norton equation (27). Figure 4 shows both a calculated stress relaxation curve obtained from the present set of formulae and a stress relaxation curve calculated by means of the Norton equation (27). The two curves confirm that the creep law involving the internal stress causes stress relaxation to a value lower than that obtained in a conventional analysis not using the internal stress concept.

5.4.2 Stress Relaxation Subsequent to Cyclic Straining

Another interesting stress relaxation effect caused by the internal stress σ_i has been described by Walker.[11] In this case the preceding experiment was not a hot tensile test or creep test but a low cycle fatigue experiment with a strain rate of $\dot{\varepsilon} = \pm\ 1.36{*}10^{-3}\,s^{-1}$ using a strain range $\Delta\varepsilon = \pm\ 0.4\%$. After steady state conditions were reached the testing machine was switched to a strain hold condition during unloading when the stress $\bar{\sigma}$ turned negative. During the subsequent phase of stress relaxation the stress was observed to rise backwards to positive values. The effect is due to the internal stress σ_i by means of the following mechanism:

- Neglecting the small amount of negative stress $\bar{\sigma}$ at the start of the relaxation experiment equation (15) shows that the negative internal stress causes a negative creep rate. However, in stress relaxation the elastic strain rate corresponds to an inverse creep rate which is positive. Thus the elastic strain and thereby the elastic stress is raised. The stress raising process continues as long as an internal stress σ_i exists and as long as it is not compensated for by the raised stress $\bar{\sigma}$.

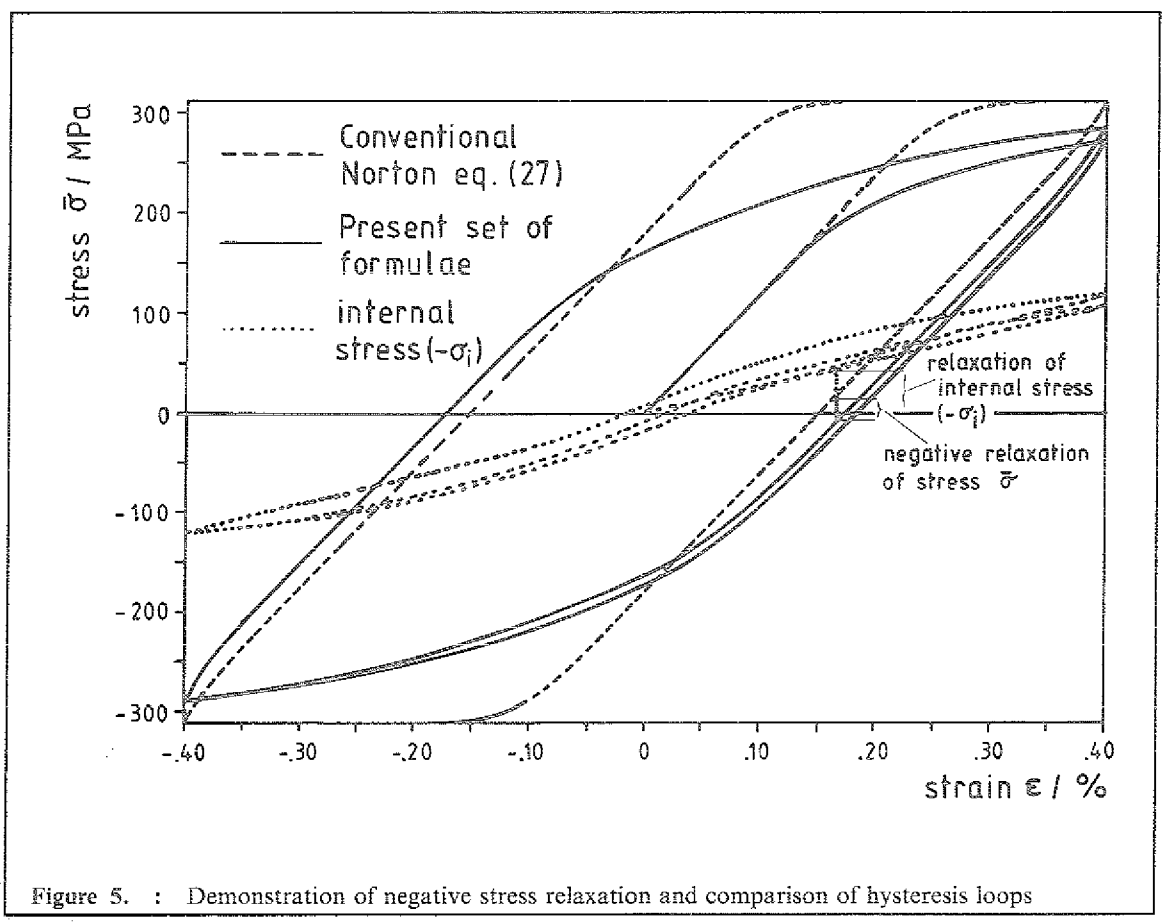

Figure 5. : Demonstration of negative stress relaxation and comparison of hysteresis loops

[11] K.P.Walker - Research and Development Program for Nonlinear Structural Modeling with Advanced Time-Temperature Dependent Constitutive Relationship, NASA-Report CR165533, Nov 1981, Figure 8.

Figure 5 shows calculated hysteresis loops for $\bar{\sigma}$, for the internal stress $-\sigma_i$ and also the hysteresis loops where $\bar{\sigma}$ was evaluated by means of the related Norton equation, equation (27), i.e. without using an internal stress but adapted to produce ultimately the same strain rates at two selected values of stress. The shapes of the two hysteresis loops for $\bar{\sigma}$ differ markedly. The effect of negative stress relaxation represented in Figure 5 by a small vertical bar occurred on the following time scale:

The zero cross-over for the stress $\bar{\sigma}$ was reached after 3 min and a maximum value in $\bar{\sigma}$ was established after 20 h.

All strain controlled calculations were performed by using the equation

$$\dot{\bar{\sigma}} = E\,(\dot{\varepsilon} - \dot{\varepsilon}^c) \tag{30}$$

and the values given in Table I. The hysteresis loops show a negligible amount of hardening. They become stationary within three cycles.

5.5 Recoverable Creep

Figure 6 shows the calculated results for a fictitious experiment with constant load rate using an applied stress rate of $\dot{\bar{\sigma}}_0 = 28790$ MPa/h. The experiment is interrupted by an unloading and reloading procedure performed at the same rate. Also, between unloading and reloading the specimen was kept free of stress for two hours. Due to a certain amount of recoverable creep strain a narrow loop is generated. With reference to the mechanism presently applied the effect of recoverable creep is caused by the relaxing internal stress in much the same way as the negative stress relaxation is caused by the internal stress, i.e. via equation (15) with no applied stress $\bar{\sigma} = 0$.

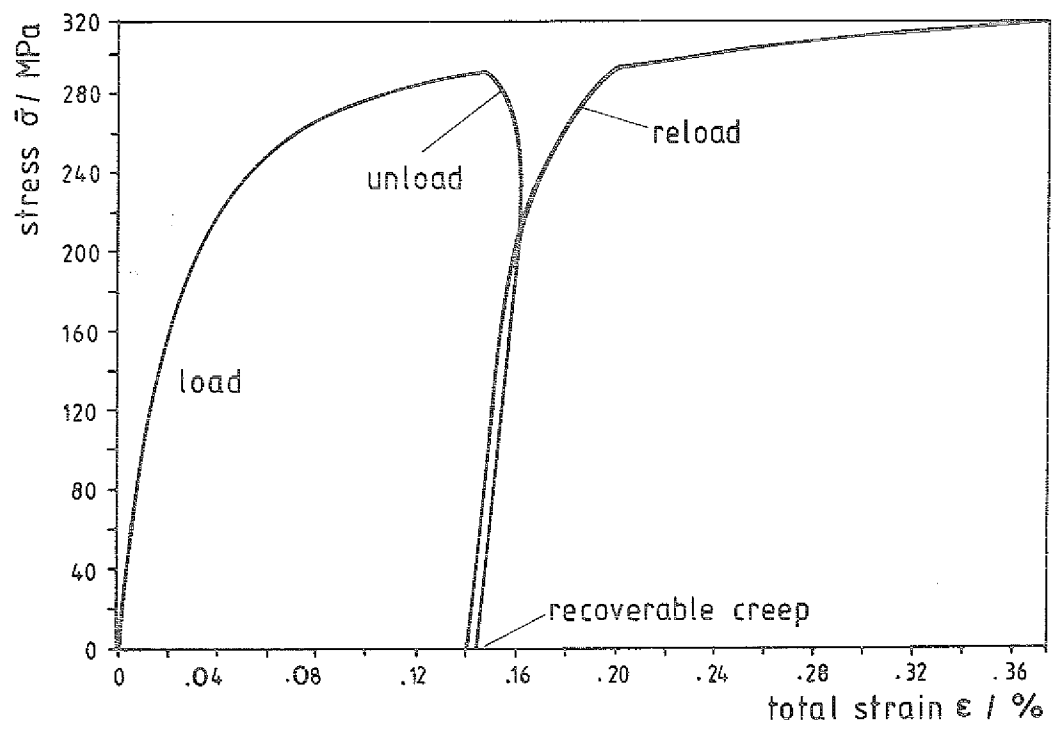

Figure 6. : Recoverable creep accumulated during a hold time which was included in a load sequence: load, unload, hold time and reload each at constant rate of stress

6.0 Plasticity

6.1 The Concept of Work Stress

The state of the isotropic continuum is defined as perfectly plastic if all admissible states of stress fulfil an isotropic condition the yield condition.[12] Physically this definition implies that at the yield limit the rate of plastic flow associated with any stress-increment would increase so rapidly that stresses greater than the yield stress cannot, in fact, be sustained.

Perfect plasticity applies to an idealized state of the material. Nevertheless for further analysis it is assumed that the state of perfect plasticity is being passed through at least temporarily. It is assumed that at the onset of plasticity the material instantaneously loses the ability for a lateral contraction constraint. Lateral contraction above the yield limit may also be considered as characterized by a Poisson's ratio $\nu = 1/2$ (see equation (10)). The assumption implies that at the yield point the material unlocks a certain amount of internal resistance against creep straining, i.e. a collapse of the internal back stress σ_i followed by the release of the corresponding amount of axial strain. The instantaneous release of axial strain is indistinguishable from any other spontaneously applied elastic stress, and it is therefore recorded by the load cell as a stress relaxation in a fashion not to reduce the measured stress but to keep it constant. The stress remains constant as long as the radial contraction constraint is not exhausted and as long as additional work is supplied by the testing machine to overcome the internal resistance (first assumption).

The other important assumption for a further theoretical analysis is the continued validity of the combined creep/relaxation law in the plastic regime (second assumption). The assumption implies that Poisson's ratio and Young's modulus as used in the creep/relaxation law are not changed when plastic effects are to be considered.

Apparently, the two assumptions are in conflict with each other and this problem will be treated first. The problem is quite obvious with respect to brittle failure:

- A stress-strain relationship usually does not include the property of brittle failure. Therefore, by continuously raising the stress it is possible to predict the stress-strain behaviour of a material specimen far beyond the limit of its individual existence. However, the physical value of stress cannot be raised continuously ad infinitum because it is measured to be zero at the point of failure. It is a fictitious stress which is being continuously raised for the purpose of predicting the material behaviour beyond the failure of an individual specimen.

A similar situation is encountered when a ductile material is stressed up to the yield limit and beyond it. A testing machine programmed to raise the stress $\bar{\sigma}$ at a constant rate fails to do so if unconditional yielding occurs. Instead the machine power is increased in order to attempt this impossible task.

It is therefore concluded that for a continuous extrapolation of the creep/relaxation law a continuous stress variable $\bar{\sigma}$ is required which differs from the physically measured stress σ. On entering the plastic regime the continuously increased stress $\bar{\sigma}$ effects a continuously increased plastic deformation by means of the creep/relaxation law while the physically measured stress σ is allowed to remain constant. For mathematical formulation the following relationship between the two stresses σ and $\bar{\sigma}$ is postulated and the postulate is in agreement with the assumptions made.

$$\sigma = \bar{\sigma} + S_t \sigma_i \tag{31}$$

This anticipated functional relationship $\sigma = \sigma(\bar{\sigma}, \sigma_i)$ is illustrated in Figure 7.

---

[12] A.M.Freudenthal and H.Geiringer, The Mathematical Theories of the Inelastic Continuum, Encyclopedia of Physics edited by S. Flügge, vol.XI, Elasticity and Plasticity, Springer, Berlin, 1958, p.278.

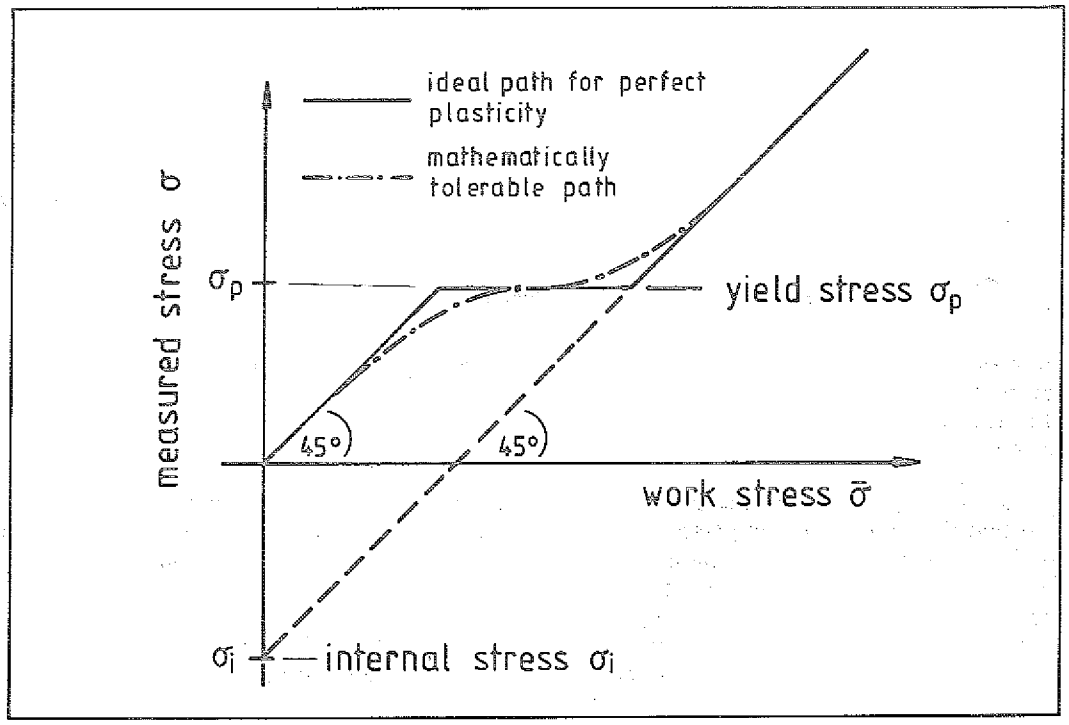

Figure 7. : Functional relationship between physically measured stress σ , work stress $\bar{\sigma}$ and internal stress σ_i .

The Figure shows that for stresses less than the yield stress σ_p, i.e. in the elastic regime, the two stresses σ and $\bar{\sigma}$ are identical. At the yield limit the physically measured stress σ remains constant while the stress $\bar{\sigma}$ is being continuously raised. The constant stress condition is maintained at the expense of the internal stress σ_i. Subsequent to the complete collapse of the internal stress σ_i it is again possible to increase both stresses σ and $\bar{\sigma}$ in a proportional relationship. The step function S_t in equation (31) has been introduced in order to model the step as shown in Figure 7. For perfectly plastic conditions the step function S_t should have the following properties:

$$S_t = \begin{cases} 0 & \sigma < \sigma_p \quad \text{elasticity} \\ 1 & \sigma \geq \sigma_p \quad \text{perfect plasticity} \end{cases} \tag{32}$$

However, yielding to both

- the demands of the numerical integration methods and
- the properties of a real material,

a continuous step function was chosen for the purpose of test calculations:

$$S_t = \frac{1}{2}\left\{1 + \tanh\left[\frac{2(\sigma + \bar{\sigma} - 2\sigma_p)}{-\sigma_i}\right]\right\} \tag{33}$$

with

$$\sigma_p = K\,\text{sign}(-\sigma_i)\,|\dot{\varepsilon}_p^c|^{1/n} - \frac{3}{4}\sigma_i. \tag{34}$$

In the present analysis the yield stress σ_p is defined by means of a limit value for plastic strain rate $\dot{\varepsilon}_p^c$. Equation (34) corresponds to equation (15) for the onset of plasticity. At the inflection point of the step function S_t, i.e. $\sigma_p = (\sigma + \bar{\sigma})/2$, the stress-stress relationship $\sigma = \sigma(\bar{\sigma}, \sigma_i)$ has a zero slope: $d\sigma/d\bar{\sigma} = 0$.

The interpretation of equation (31) is not yet complete. In particular, a physical meaning of the continuously increasing stress function $\bar{\sigma}$ is missing. This can be achieved by integrating equation (31) with respect to the total strain ε :

$$\int_{\varepsilon_1}^{\varepsilon_2} \sigma \, d\varepsilon = \int_{\varepsilon_1}^{\varepsilon_2} \overline{\sigma} \, d\varepsilon + \int_{\varepsilon_1}^{\varepsilon_2} S_i \sigma_i \, d\varepsilon. \tag{35}$$

The relationship equation (35) accounts for various work terms. The left hand side term

$$W_p = \int_{\varepsilon_1}^{\varepsilon_2} \sigma \, d\varepsilon \tag{36}$$

accounts for the elastic strain energy if the stress σ is less than the yield stress σ_p. It accounts for the plastic strain work for stresses greater than the yield stress σ_p and it is known to be zero for plastic strain work done on the yield surface in the case of perfect plasticity.[13] The last term in equation (35)

$$W_i = \int_{\varepsilon_1}^{\varepsilon_2} S_i \sigma_i \, d\varepsilon \tag{37}$$

represents the work necessary to supersede the material's internal resistance to creep. In the case of perfect plasticity internal work W_i is only done if plastic conditions are reached.

The remaining term in equation (35)

$$W = \int_{\varepsilon_1}^{\varepsilon_2} \overline{\sigma} \, d\varepsilon \tag{38}$$

represents the total external work done by the testing machine. In an experiment with constant load rate, the external work W

- initially supplies elastic strain energy
- secondly supplies the necessary work to overcome the internal resistance and
- thirdly, in the case of strain hardening, is used to increase further the strain energy.

According to equation (38) the derivative of the total external work with respect to the strain is

$$\overline{\sigma} = \frac{dW}{d\varepsilon}. \tag{39}$$

The stress $\overline{\sigma}$ is a stress related to the increase of external work W necessary to obtain an increase in strain ε. It will be therefore called work stress.

6.2 Strain Hardening in Strain Rate Controlled Experiments

A typical stress-strain behaviour in hot tensile testing is shown for instance by Schubert et al.[14] As a result of a strain controlled experiment with constant strain rate, a tri-linear stress-strain behaviour is observed in many cases. In the elastic region the stress grows linearly with the applied strain ε, approximately following Hooke's law, $\sigma = E\varepsilon$. On entering the plastic regime the stress-strain curve instantaneously changes to another constant slope until equilibrium conditions are reached when all of the applied strain ε supplied per time unit is converted into plastic strain. Under such conditions the stress σ remains constant. The problem of a tri-linear stress-strain behaviour has also been studied by Miller, Hart, Krieg, Swearengen and Rohde and has been referenced by Walker.[15]

---

[13] A.M.Freudenthal and H.Geiringer, The Mathematical Theories of the Inelastic Continuum, Encyclopedia of Physics edited by S. Flügge, vol.XII, Elasticity and Plasticity, Springer, Berlin, 1958, p.278.

[14] F.Schubert, H.H.Over and H.Nickel, Principles for Structural Design Codes for Components in the Creep Temperature Region mainly above 800^0 C , Proceedings of the International Conference on CREEP, April 14-18, 1986, Tokyo p.p. 539-543, Figure 6

[15] K.P.Walker - Research and Development Program for Nonlinear Structural Modeling with Advanced Time-Temperature Dependent Constitutive Relationship, NASA-Report CR165533, Nov 1981, Figure 9.

In the present analytical approach, it was found most effective to include the described strain hardening effect in the definition of the elastic strain. The phenomenological appearence of the measured stress-strain curve is such that the assumption of a Young's modulus specific for the plastic regime is rather tempting. The development is not unique and may be compared with the introduction of an asymptotic tangent modulus E_t as used by Krempl.[16]

Conversely, the studies on the introduction of a plastic Young's modulus done by Krempl [16] show that complex logical decisions necessarily have to be imposed if the loading is not applied unidirectionally. On load reversal a plastic Young's modulus is not observed indicating that this effect is plastic in nature, and for this reason it does not seem to be advantageous to combine the effect of strain hardening with a term which otherwise is purely elastic in nature.

Nevertheless, also in the present development the possibility of a plastic Young's modulus was studied. It was introduced to be effective only above a certain limit of strain rate $\dot{\varepsilon}_h^c$ and only on loading. Furthermore, it was introduced only to affect the elastic strain but not the combined stress-relaxation law. The complete definition of the elastic strain rate is

$$\dot{\varepsilon}^{el} = \frac{\dot{\sigma}}{(1 - S_h)E + S_h E_h} \tag{40}$$

with

$$S_h = \frac{1}{4}\left\{1 + \tanh\left[\alpha(|\dot{\varepsilon}^c| - \dot{\varepsilon}_h^c)\right]\right\}\{1 + \tanh(\alpha x)\} \tag{41}$$

and $$x = \begin{Bmatrix} \sigma\,\dot{\sigma} & \text{if controlled by measured stress} \\ \overline{\sigma}\,\dot{\overline{\sigma}} & \text{if controlled by work stress} \\ \sigma\,(\dot{\varepsilon} - \dot{\varepsilon}^c) & \text{if controlled by strain} \end{Bmatrix}.$$

The switch function S_h, equation (41), causes Young's modulus $\overline{E}$ to be evaluated according to the above mentioned condition. The more general equation (40) replaces equation (12). The parameter α effects a transition sufficiently smooth to be accepted by the numerical algorithm. Above the yield limit the measured stress rate $\dot{\sigma}$ in equation (40) is influenced by the internal stress σ_i (see equation (31)).

The limit value for strain hardening $\dot{\varepsilon}_h^c$ is initially chosen to be identical with the plastic yield limit $\dot{\varepsilon}_p^c$. However, once $\dot{\varepsilon}_p^c$ is surmounted by the current value of strain rate $\dot{\varepsilon}^c$ the limit value for strain hardening is replaced by the maximum value in strain rate recorded, i.e.

if $[S_h > 0]$ then $[\dot{\varepsilon}_t^c = \max(|\dot{\varepsilon}^c|, \dot{\varepsilon}_h^c)]$ else $[\dot{\varepsilon}_h^c = \dot{\varepsilon}_t^c]$.

$\dot{\varepsilon}_t^c$ is a quantity provided for temporary storage.

Usually the strain hardening effect is counteracted by the process of thermal or dynamic recovery which so far has not been included in the present formulation of a hardening rule.

6.3 Various Experimental Controls

Experiments to study creep and plastic effects are invariably performed either in strain or in stress control. Due to the present development a third possibility can be anticipated, i.e. an experiment controlled by the work stress $\overline{\sigma}$ as defined by equation (39). The three experiment types are discussed subsequently.

6.3.1 Experiments Controlled by Stress

The superposition of elastic strain rate, equation (40), and inelastic strain rate, equation (15), provides a total strain rate

---

[16] E.Krempl, J.J.McMahon, D.Yao - Viscoplasticity Based on Overstress with a Differential Growth Law for the Equilibrium Stress, NASA Symposium, Cleveland, Ohio, June 13-15, 1984, Table 1 & 2

$$\dot{\varepsilon} = \dot{\varepsilon}^c + \frac{\dot{\sigma}}{(1 - S_h)E + S_h E_h}. \tag{42}$$

A stress controlled experiment can be simulated by an appropriate definition of a function $\dot{\sigma} = \dot{\sigma}(t)$. If the experiment is not controlled by the true stress σ but instead by a load stress σ_0, then the true stress σ and its time derivative $\dot{\sigma}$ have to be calculated by using one or both of the following equations

$$\sigma = \sigma_0 e^{\varepsilon^c} \tag{43}$$

and

$$\dot{\sigma} = \dot{\sigma}_0 e^{\varepsilon^c} + \sigma \dot{\varepsilon}^c. \tag{44}$$

The corrections given by the equations (43) & (44) were applied to all of the calculations.

6.3.2 Experiment Controlled by External Work

In using the work stress $\bar{\sigma}$ as a primarily controlled input function, an additional relationship $\dot{\sigma} = \dot{\sigma}(\bar{\sigma})$ is required. In order to avoid too complex functional relationships an approximate function was defined

$$\dot{\sigma} = \frac{(2S_t - 1)^2}{2 - (2S_t - 1)^2} \dot{\bar{\sigma}}. \tag{45}$$

Equation (45) represents the slope of the function $\sigma = \sigma(\bar{\sigma})$ as represented in Figure 7, neglecting the fact that the internal stress σ_i implicated in the step function S_t implicitly depends on time. $\dot{\sigma}$ obtained from equation (45) is substituted for $\dot{\sigma}$ in equation (42) thereby not inflicting any changes upon the integrated relationship $\sigma = \sigma(\bar{\sigma})$ given by equation (31). Thus, in exerting control via the work stress, equation (42) is replaced by

$$\dot{\varepsilon} = \dot{\varepsilon}^c + \frac{\dfrac{(2S_t - 1)^2}{2 - (2S_t - 1)^2}}{(1 - S_h)E + S_h E_h} \dot{\bar{\sigma}}. \tag{46}$$

For the subsequent calculations a constant load stress rate $\dot{\bar{\sigma}}_0$ was simply assumed and corrected for lateral contraction by means of the equations (43) & (44). In actual experiments $\bar{\sigma}$ and $\dot{\bar{\sigma}}$ have to be derived and controlled in real time time analysis via equation (39).

6.3.3 Experiments Controlled by Strain

The relationship equation (42) reformulated explicitly for $\dot{\sigma}$ and additionally corrected for lateral contraction results in

$$\dot{\sigma}_0 = [(1 - S_h)E + S_h E_h] e^{-\varepsilon^c} (\dot{\varepsilon} - \dot{\varepsilon}^c) - \sigma_0 \dot{\varepsilon}^c. \tag{47}$$

If the experiment is not directly controlled by the true strain ε but by the technical strain then additional relationships

$$\varepsilon = \ln|1 + \varepsilon_0| \tag{48}$$

and

$$\dot{\varepsilon} = \frac{\dot{\varepsilon}_0}{(1 + \varepsilon_0)} \tag{49}$$

are required. A unique definition of the system of simultaneous equations was found possible only if the definition of loading or unloading was introduced as depending on the load case (see variable x in equation (41)).

7.0 Simulated Experiments with Loads Exceeding the Yield Limit

7.1 Experiments Controlled by Work Stress

For further study of the present theoretical approach a simulated experiment performed at constant rate of work stress $\dot{\bar{\sigma}}_0$ is of primary interest. The result of such a calculation is shown in Figure 8. Three stress-strain curves are presented in one diagram; they are the work stress $\bar{\sigma}$, the effective stress $\bar{\sigma} + \sigma_i$ and the measurable stress $\sigma = \bar{\sigma} + S_i\sigma_i$. The stress rate selected for the demonstration was $\dot{\bar{\sigma}}_0 = 20.48$ MPa/h. All other constants necessary for performing the calculation are specified in Tables I-II.

Table II : Values chosen for numerical studies concerning plasticity	
plastic strain rate yield limit	$\dot{\varepsilon}_p^c = 0.052\ \mathrm{h}^{-1}$
plastic Young's modulus	$E_h = 1613$ MPa
promptitude of switch	$\alpha = 1000$ h

For the purpose of calculations with stresses exceeding the yield stress the drag stress previously set to $K = 133.7$ MPa (Table I) was increased to a value $K = 300$ MPa. The intention was to decelerate the plastic deformation process above the yield limit. Thus, a more moderate material response is attained at the plasticity limit in comparison with the results from creep calculation presented in Section 5.

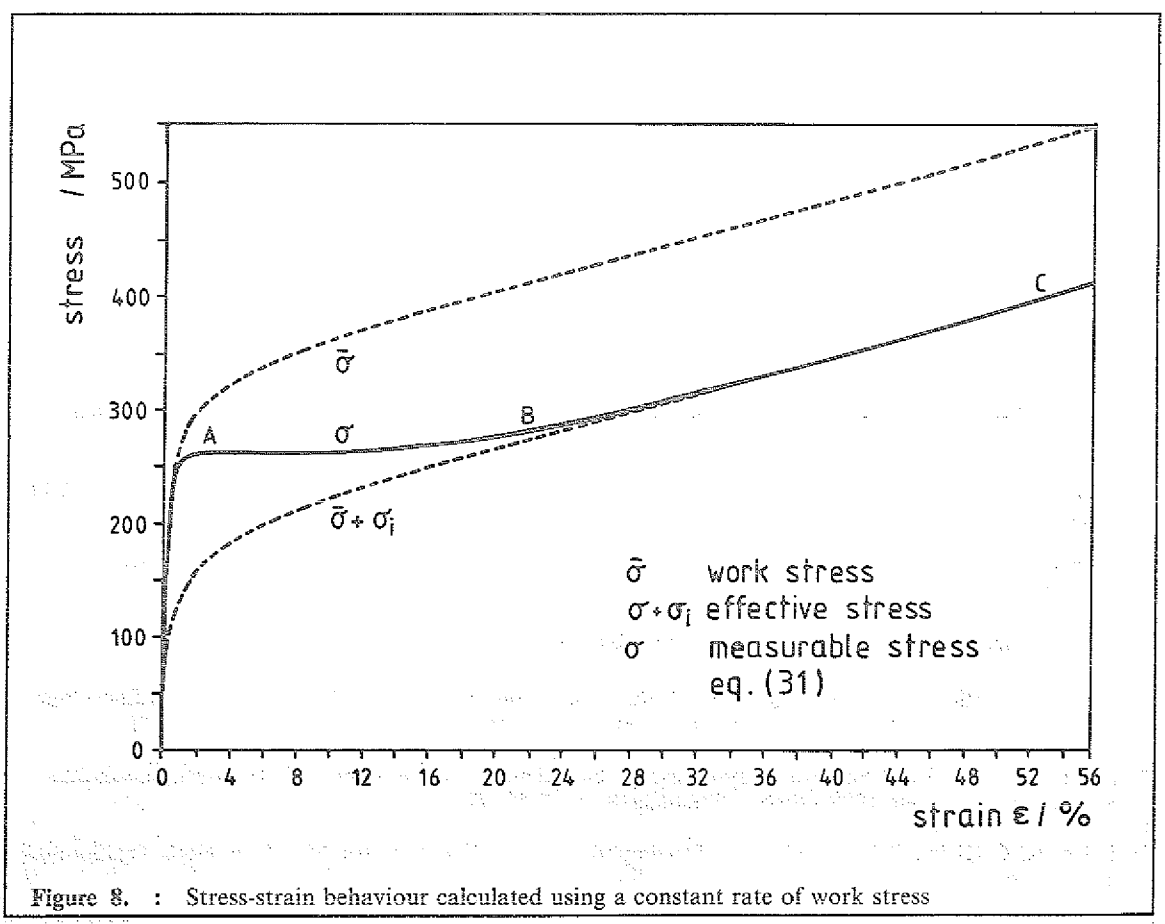

Figure 8. : Stress-strain behaviour calculated using a constant rate of work stress

The description of a typical stress-strain behaviour is given by Timoshenko.[17] His representation of experimental facts is subsequently quoted and it fully applies to the present results:

- To explain the sudden stretching of steel at its yield point A (see Figure 8), it has been suggested by Ludwik et al.[18] that the boundaries of the grains consist of brittle material and form a rigid skeleton which prevents plastic deformation of the grains at low stress. Without such a skeleton the tensile test diagram would be like that indicated in Figure 8 by the broken line labelled $\bar{\sigma} + \sigma_i$. Due to the presence of the rigid skeleton, the material remains perfectly elastic and follows Hooke's law up to point A, where the skeleton breaks down. Then the plastic grain material suddenly obtains the permanent strain AB, after which the material follows the usual curve BC i.e. $\bar{\sigma} + \sigma_i$ for a plastic material.

Although the so-called skeleton theory nowadays is superseded by more modern concepts based on the properties of dislocation lines it remains the fact that a proper phenomenological description of experimental evidence is given on the grounds of a heterogenious material behaviour. For the present purpose it is irrelevant whether the heterogeneity is caused by the boundaries of grains or by dislocation lines with the properties of being sessile in parts of the material and being mobile in other parts of the same material.

The measured stress-strain curve is sometimes complemented by a yield point effect showing an upper and lower yield point with a fast intermediate transition, $d\sigma/d\varepsilon < 0$.[19] The effect is believed to be directly related to an initial lack of mobile dislocation lines.[20,21,22] A theoretical approach to model the yield point effect on account of dislocation lines has been described also by the authors.[23]

Another effect is due to be discussed in relation to Figure 8, i.e. the properties of the stress-strain relationship at high temperatures when the yield point is known to disappear gradually. For demonstration purposes the plastic strain rate yield limit $\dot{\varepsilon}_p^c$ was chosen to have point A of Figure 8 located such that a yield point is clearly shown. Obviously, in reducing the value for the plastic strain rate yield limit $\dot{\varepsilon}_p^c$, point A would be shifted to lower values of stress such that the characteristic behaviour of the stress-strain curve at the yield point would gradually disappear. Apparently the heterogeneous properties of the material presently seen as the main cause for the existence of a yield point are less pronounced at high temperatures.

The results from a calculation similar to the one shown in Figure 8 but including unloading and reloading paths are shown in Figure 9. Loading and unloading/reloading in a first cycle was caused at a rate $\dot{\bar{\sigma}}_0 = 2.56$ MPa/h and $\dot{\bar{\sigma}}_{01} = 171.52$ MPa/h respectively.

---

17 S. Timoshenko - Strength of Materials, part II, Advanced Theory and Problems, D. van Nostrand Comp.Inc, New York, 1956, p.419

18 P.Ludwik and Scheu, Werkstoffausschuß Ver.deut.Ing.Ber, No 70, 1925; W.Köster, Archiv Eisenhüttenwesen, No 47, 1929

19 S. Timoshenko - Strength of Materials, part II, Advanced Theory and Problems, D. van Nostrand Comp.Inc, New York, 1956, p.417

20 A.H.Cottrell and V.Ayetkin, J.Inst. Met. 77 (1950) 413

21 A.M.Freudenthal and H.Geiringer, The Mathematical Theories of the Inelastic Continuum, Encyclopedia of Physics edited by S. Flügge, vol.XI, Elasticity and Plasticity, Springer, Berlin, 1958, p.278.

22 P.Paufler and G.E.R.Schulze, Physikalische Grundlagen mechanischer Festkörpereigenschaften II, Vieweg Braunschweig 1978, ISBN 3 528 068418, p. 37-42, 72

23 H.Cords, G.Kleist, R.Zimmermann - Development of a Creep Law for Metals at High Temperatures, Transactions of the 8th International Conference on Structural Mechanics in Reactor Technology, Brussels, Belgium, Aug 19-29, 1985, Vol L 6/3 p.287

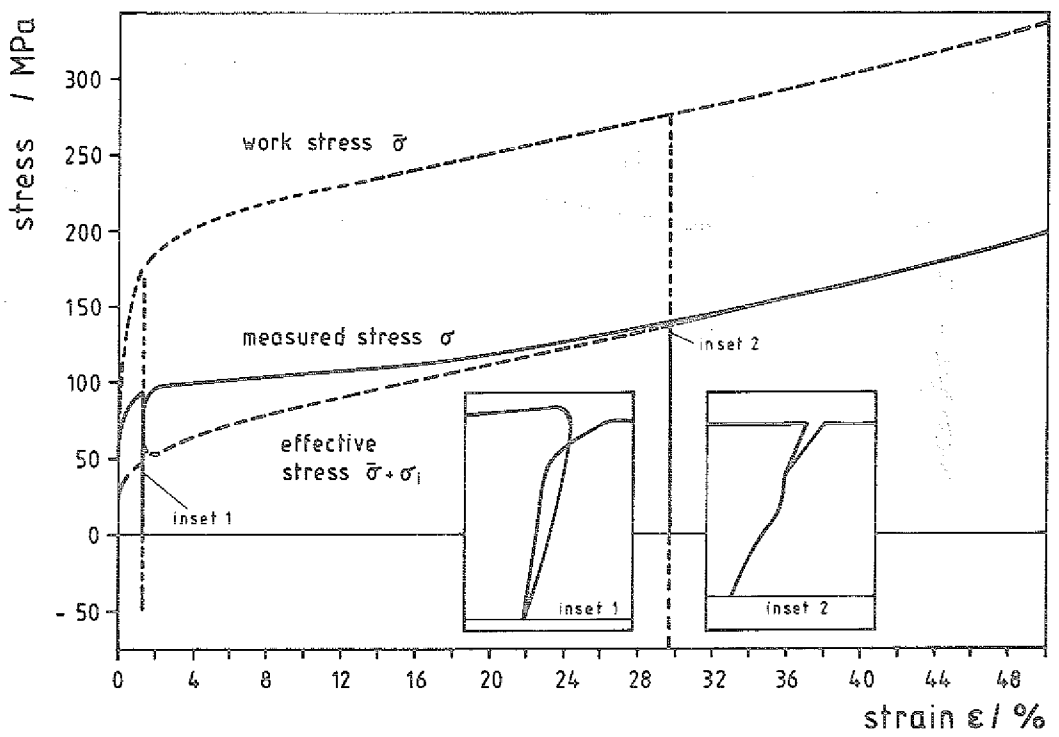

Figure 9. : Stress-strain relationship with two unloading/reloading paths included at different levels of strain rate.

The first unloading and reloading path forms a narrow loop (see first inset in Figure 9) indicating that a certain amount of strain is recoverable. The effect is anelastic by nature[24] considering the short time scale during which recovery occurs. The loop vanishes if unloading is started at a much higher inelastic strain rate (see second inset in Figure 9). A much higher stress rate $\dot{\bar{\sigma}}_{02}$ = 204928 MPa/h used during unloading and reloading could not compensate for the loss of the loop. Instead, at this high stress rate the magnification shows a deviation from linearity the cause of which could not be cleared but may possibly be connected to the approximate character of equation (45).

Figure 10 depicts the theoretical stress-strain behaviour of the material for a number of constant stress rates spaced at equal distance on a logarithmic scale.

[24] A.M.Freudenthal and H.Geiringer, The Mathematical Theories of the Inelastic Continuum, Encyclopedia of Physics edited by S. Flügge, vol.XI, Elasticity and Plasticity, Springer, Berlin, 1958, p.263.

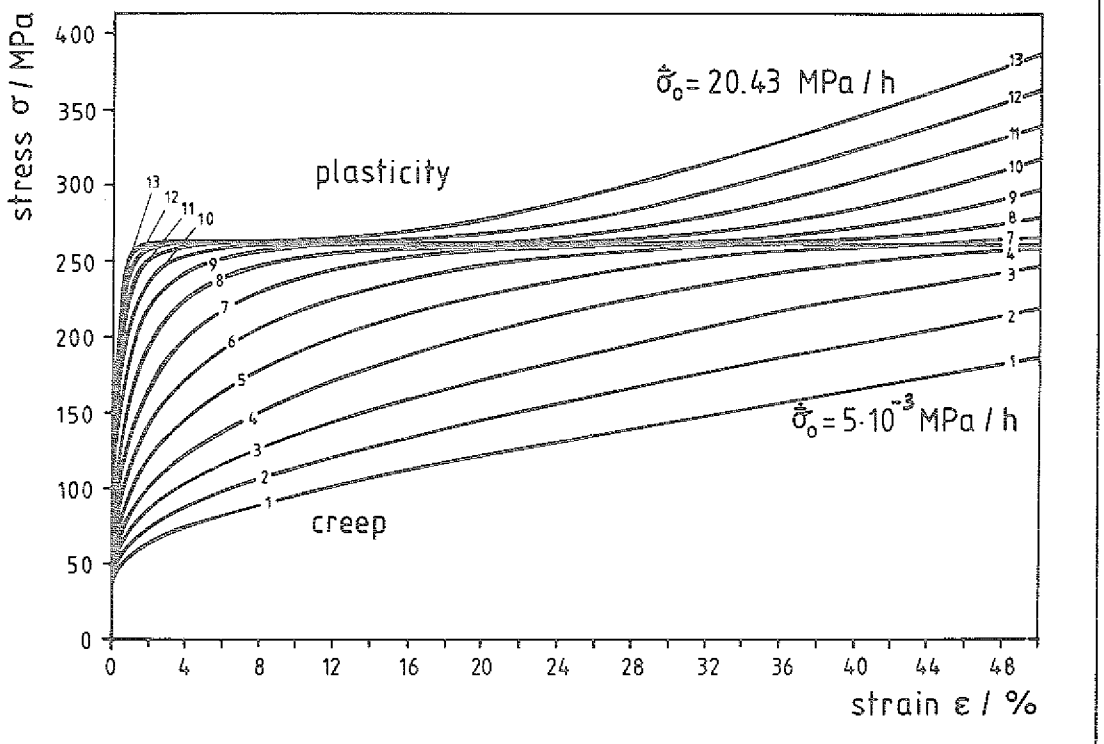

Figure 10. : Stress-strain relationship calculated for various, constant rates of work stress $\bar{\sigma}_0$ - The numerals n = 1,2,...13 attached to each of the curves refer to constant stress rates $\dot{\sigma}_0 = 2.5*10^{-3}*2^n$.

There are three categories

- At low loading rates ($\dot{\bar{\sigma}}_0$ = constant) the yield limit is reached after a relatively long time during which a considerable amount of creep strain is accumulated. Accordingly, the slope of the stress-strain curve $\sigma = \sigma(\varepsilon)$ is low.
- At medium loading rates ($\dot{\bar{\sigma}}_0$ = constant) the yield limit is reached more quickly but it is not immediately surmounted at low strains.
- At high loading rates the intermediate state of the material during which it becomes fully plastic is passed through quickly, releasing only a small amount of creep strain during that time.

7.2 *Experiments Controlled by Stress*

As discussed in Section 6.1, the load stress σ_0 measured by a load cell in line with the specimen cannot be controlled completely for technical reasons. If unconditional yielding occurs, at best the measured stress is found to be constant although the testing machine was programmed to raise the stress σ at a constant rate. As it appears from the present work, stress control in testing is experimentally ill-defined. Therefore it is conceivable that the experimental testing conditions actually are intermediate to the two theoretical cases of stress control presently discussed i.e. control by work stress and control by measurable stress.

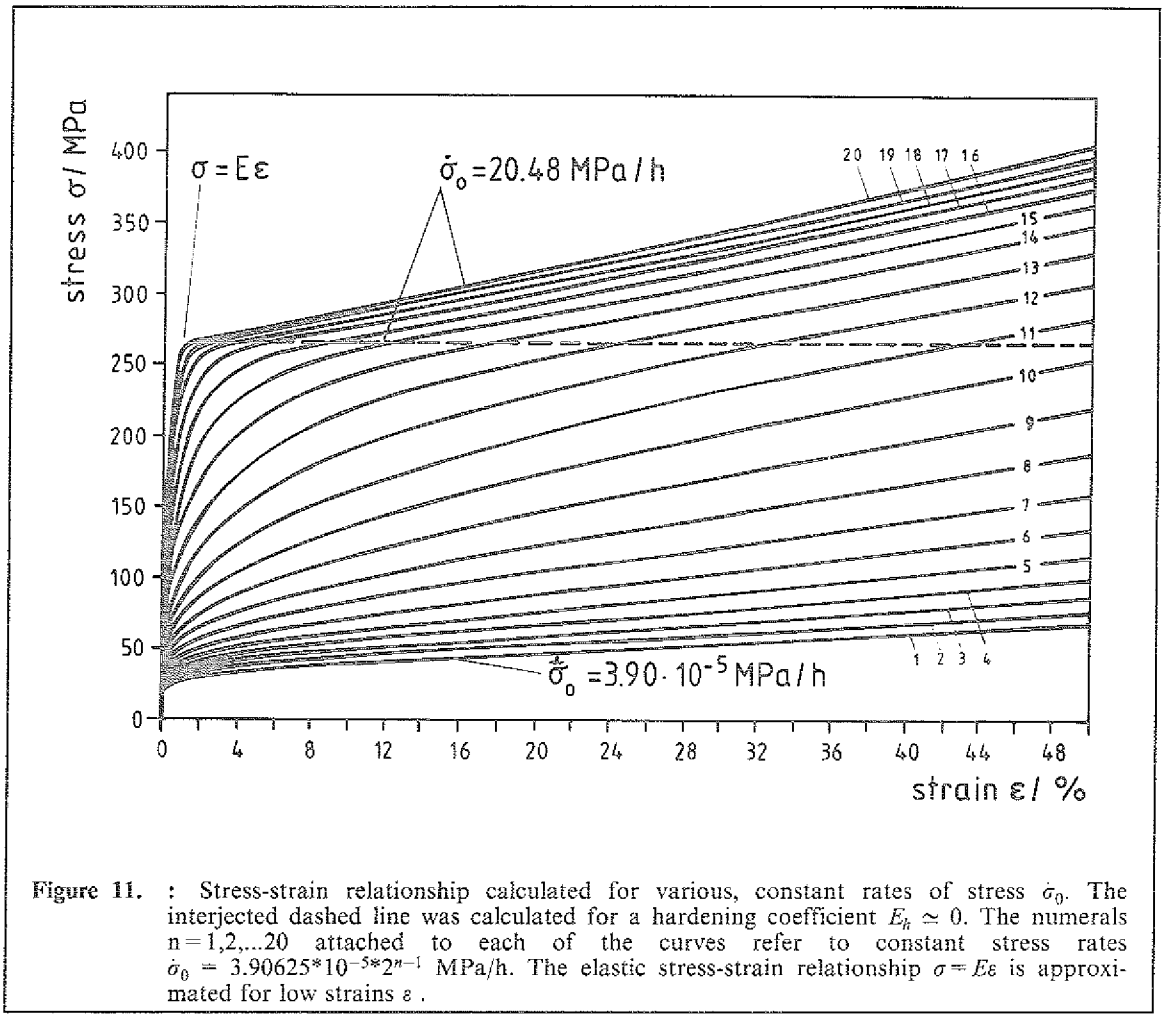

Figure 11. : Stress-strain relationship calculated for various, constant rates of stress $\dot{\sigma}_0$. The interjected dashed line was calculated for a hardening coefficient $E_h \simeq 0$. The numerals n = 1,2,...20 attached to each of the curves refer to constant stress rates $\dot{\sigma}_0 = 3.90625*10^{-5}*2^{n-1}$ MPa/h. The elastic stress-strain relationship $\sigma = E\varepsilon$ is approximated for low strains ε .

The corresponding theoretical calculation for a control by measurable stress can be performed without difficulties. Figure 11 shows the results of calculations for a number of simulated experiments each performed at constant rate of stress, $\dot{\sigma}_0 = \text{const}$ using partly the same rates as the ones used for Figure 10. The diagram further shows that the yield point as introduced by equation (31) and illustrated in Figure 7 is overridden. The initial part of the set of curves is characterized by the elastic stress-strain relationship $\sigma = E\varepsilon$ serving as an envelope, while the final part is characterized by a slope which is nearly the same for high stress rates $\dot{\sigma}_0$. The common slope is related to the hardening coefficient E_h, because an additional calculation performed at the highest stress rate $\dot{\bar{\sigma}}$ = 20.48 MPa/h and using a hardening coefficient $E_h \simeq 0$ provides a stress-strain relationship typical for a perfectly plastic material behaviour. In comparing Figures 10 and 11, it can be noted that the stress-strain curves well below the yield limit, i.e. for low stress rates and particularly for $\dot{\bar{\sigma}}_0 = \dot{\sigma}_0 = 5*10^{-3}$ MPa/h, are identical. The diagram (Figure 11) is reminiscent of a similar one discussed by Krempl,[25] who postulates a lower limit for all of the stress-strain curves being an equilibrium curve for infinitely slow application of load. As it appears from Figure 11, the existence of such an asymptotic behaviour is supported but with the slope $d\sigma/d\varepsilon$ being zero for most of the time.

[25] E. Krempl - The Role of Servocontrolled Testing in the Development of the Theory of Viscoplasticity Based on Total Strain and Overstress, Mechanical Testing for Deformation Model Development, ASTM STP 765, R.W. Rohde and J.C. Swearengen, American Society for Testing and Materials, 1982, pp. 5-28

7.3 *Experiment Controlled by Strain*

7.3.1 Hot Tensile Testing - Serration

A series of calculations was performed using constant strain rates $\dot{\varepsilon}$, Figure 12.

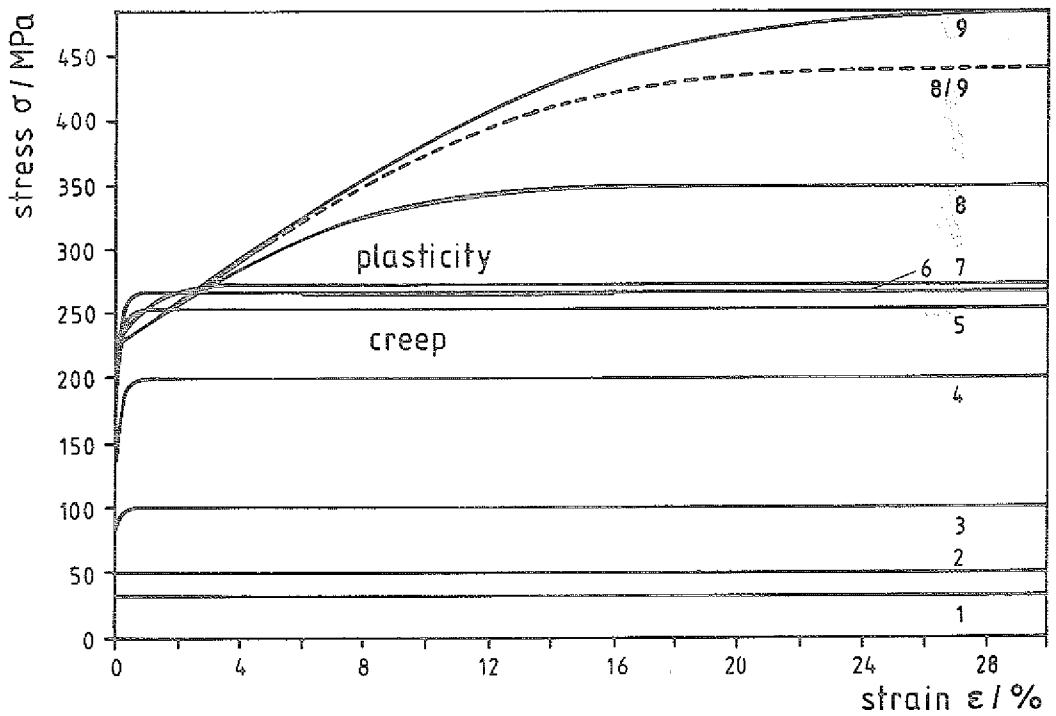

Figure 12. : Stress-strain relationship calculated for various constant strain rates equally spaced on a logarithmic scale. The numerals n = 1,2,...9 attached to each of the curves refer to constant strain rates $\dot{\varepsilon}_n = 3*10^{n-8}\ h^{-1}$. The interjected curve refers to a constant strain rate $\dot{\varepsilon}_{8/9} = 15\ h^{-1}$.

Above the yield limit ($\dot{\varepsilon}_p^c = 0.052 h^{-1}$) the stress increases linearly with a characteristic slope until the maximum stress is reached when equilibrium conditions are established. In Figure 12 the concentration of curves at the yield limit is higher than elsewhere, i.e. plastic yielding has to be compensated for by an unusually large increase in applied strain rate in order to raise the stress σ above the limit. Due to the fact that the yield criterion is based on a critical strain rate $\dot{\varepsilon}_p^c$ rather than on a yield stress σ_p (equation (34)), a stress reversal is indicated by Figure 12 close to the yield limit and at low strains.

- The creep stress at its highest level is found to be greater than the plastic flow stress recorded at the onset of plastic yielding.

Of course the statement is founded on the present theoretical approach, because only then is it possible to differentiate between creep stress and flow stress on such a narrow basis. Also theoretically, the effect is easily explained by the properties of a Maxwell body[26] which allows for stress relaxation to occur when there is a burst of plastic strain.

---

[26] M.Reiner, Rheology, Encyclopedia of Physics edited by S.Flügge, vol VI, Elasticity and Plasticity, Springer, Berlin 1958, p. 465

The phenomenon if observed experimentally is referred to as the effect of "negative strain rate sensitivity" and this effect is often associated with the Portevin - Le Chatelier effect.[27] A plot of flow stress (creep stress) versus strain rate (Figure 13) is usually performed to show the negative strain rate sensitivity and such a plot can also be derived from Figure 12.

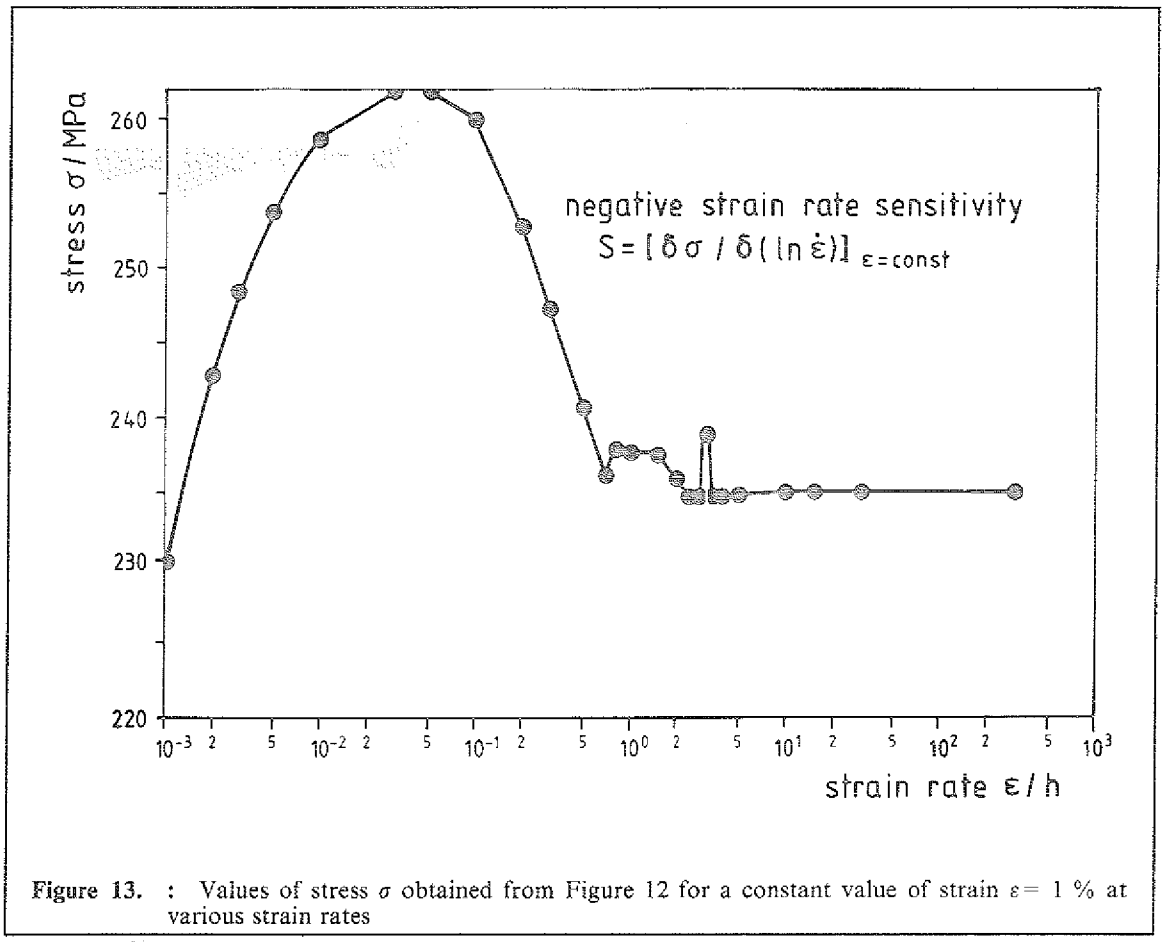

Figure 13. : Values of stress σ obtained from Figure 12 for a constant value of strain $\varepsilon = 1$ % at various strain rates

The strain rate sensitivity $S = (\partial\sigma/\partial \ln\dot{\varepsilon})_{\varepsilon=\text{const}}$ is the slope of the curve shown in Figure 13. A return of a positive strain rate sensitivity at very high strain rates is not reproduced in the calculations. Also, the calculated hot tensile stress-strain curves are not serrated where negative strain rate sensitivity is detected. Serrations would require instability which in the present development has been avoided by not simulating an ideal step function in the stress-stress relationship $\sigma = \sigma(\bar{\sigma})$, equations (31-34). The repeated occurrence of instability such as the one observed in serrated flow can possibly be caused by resolving the ideal step function (Figure 7) into a series of smaller but still ideal steps. Such a development is not warranted if it is aimed at a constitutive equation for applications in continuum mechanics.

The kind of instability expected from an ideal step function or a series of ideal steps is contained indicatively in the present theoretical approach.

- If magnified all of the calculated stress-strain curves are found to be serrated due to instabilities of the numerical algorithm used for integration of the set of simultaneous differential equations. However, if by special choice of an applied strain rate $\dot{\varepsilon} = \dot{\varepsilon}_p^c$ the stress-stress relationship $\sigma = \sigma(\bar{\sigma})$ as shown in Figure 7 is addressed at its inflection point, the numerical instabilities become a maximum because $\partial\sigma/\partial\bar{\sigma} = 0$ at this point.

To illustrate the described effect of instability which occurs directly on the yield limit the stress-strain curve $\dot{\varepsilon} = \dot{\varepsilon}_p^c$ was calculated and is presented in Figure 14 on a magnified scale. The same stress-strain relationship included in Figure 12 would not reveal serrations on that scale.

---

[27] L.P.Kubin, Y.Estrin - A nonlinear aspect of crystal plasticity: the Portevin - Le Chatelier effect, J.Physique 47 (1986) 497-505

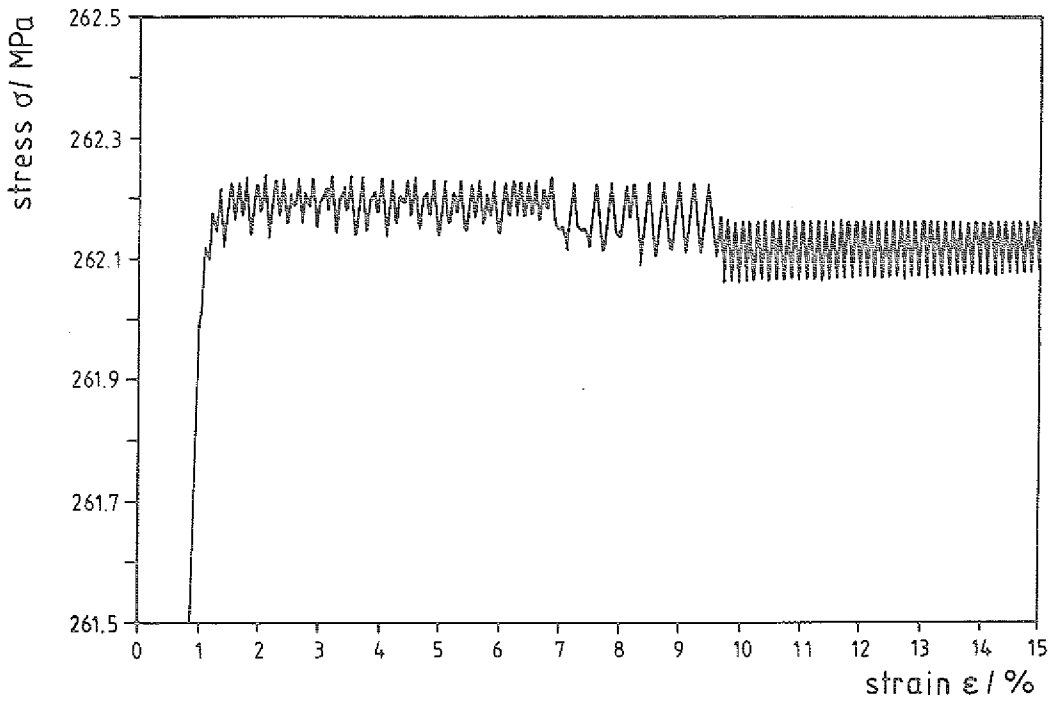

Figure 14. : Stress-strain relationship calculated in strain control at the plastic strain rate yield limit $\dot{\varepsilon} = \dot{\varepsilon}_p^c$. A small interval of stress $\Delta\sigma$ was selected to show the serrated flow at the yield limit.

7.3.2 Cyclic Loading Conditions

The material properties of 304 stainless steel at high temperatures under cyclic loading have been described e.g. by J.R.Corum et al. [28] The two current concepts for cyclic hardening are explained in Figure 23 of their publication. The calculations performed in the present investigation using the hardening rules of Section 6.2 and using the parameters given in the two Tables I and II provided results which ideally correspond to the schematic representation of the so-called isotropic hardening model (Figure 15 ; After completing the present report it was found that the corresponding calculations were done with two different values for α in equation (41). That value for α associated with the strain rates was mistakingly set to α = 100 h causing some quantitative but no qualitative changes to the figure.)

[28] J.M.Corum, W.L.Greensteet, K.C.Liu, C.E.Pugh, R.W.Swindeman - Interim Guidelines for Detailed Inelastic Analysis of High-Temperature Reactor System Components, Oak Ridge National Laboratory, ORNL - 5014, Dec 1974

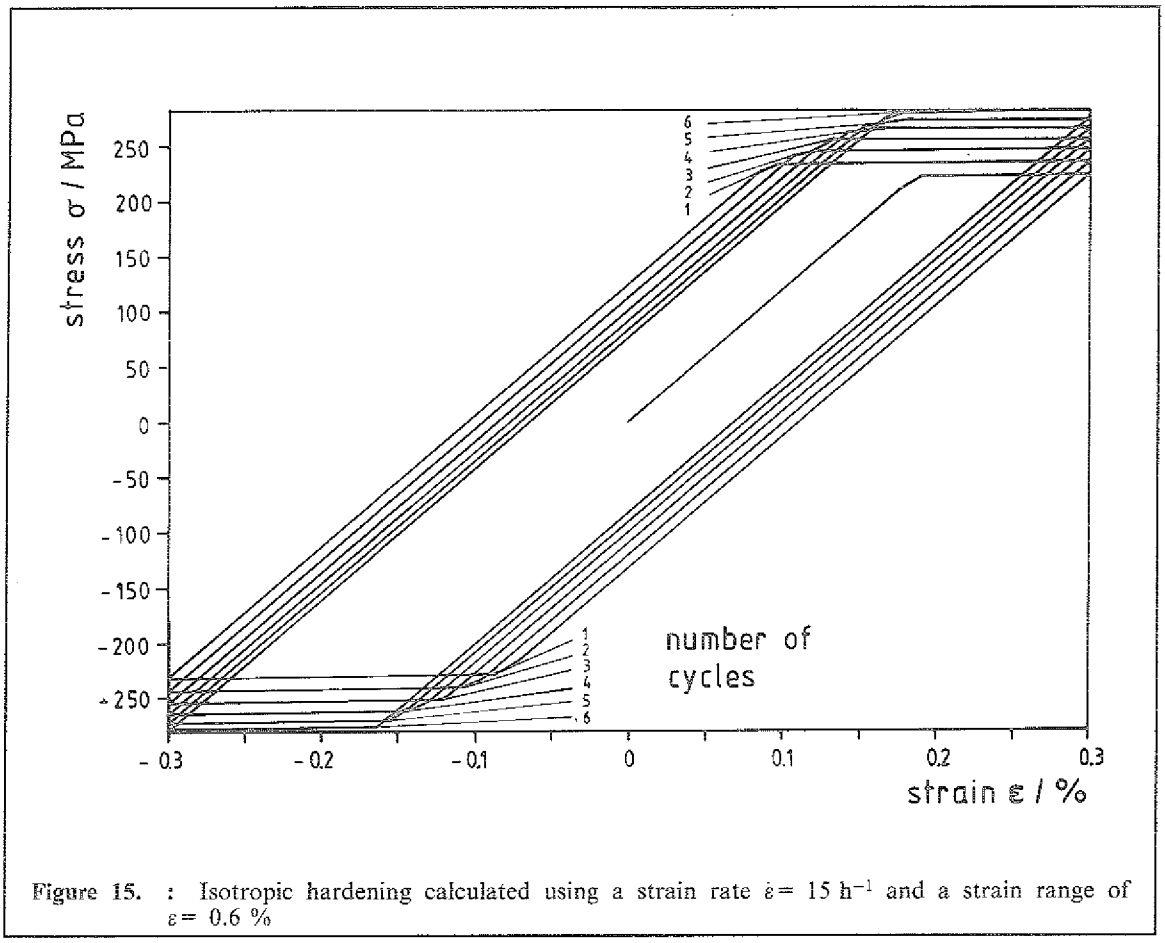

Figure 15. : Isotropic hardening calculated using a strain rate $\dot{\varepsilon} = 15\ h^{-1}$ and a strain range of $\varepsilon = 0.6\ \%$

In the present model cyclic hardening is achieved by the following procedure :

- During the first quarter-cycle the stress-strain behaviour is the same as the one shown in Figure 12 for the corresponding strain rate $\dot{\varepsilon} = 15\ h^{-1}$. Because of the small strain range at maximum stress, it is difficult to notice the small increase of stress caused by the plastic Young's modulus ($E_p < E$) over that range. The high strain rate at maximum stress $\dot{\varepsilon}^c$ exceeds the elastic limit of strain rate $\dot{\varepsilon}_h^c$ (equations (40-42)) initially set to be equal to the strain rate at the yield limit $\dot{\varepsilon}_p^c$. Therefore, for subsequent cycles, the elastic limit value $\dot{\varepsilon}_h^c$ is increased (hardening rule in Section 6.2). During the next half-cycle (see equation (47)) the absolute value of stress is raised higher than in the previous cycle; i.e. the switch function S_h causes an extended range of stress in the elastic region. The increased stress σ causes an increased strain rate $\dot{\varepsilon}^c$ such that the process repeats cycle by cycle. Termination of the hardening process can be attributed to either one of the following two cases:
  - The plastic strain rate $\dot{\varepsilon}^c$ matches the applied strain rate $\dot{\varepsilon}$.
  - The material becomes completely elastic within the strain range chosen.

The present method to include a numerical algorithm for material hardening is not dissimilar to the one briefly described by Timoshenko[29] and originally introduced by Orowan.[30] The increment of stress due to hardening can cycle by cycle be related to an increase in stress following the corresponding stress-strain curve obtained for monotonic loading as shown in Figure 12. This property is partly revealed by Figure 9 when after passing through an unloading/reloading path the range of elastic stress is obviously extended. Mechanisms such as the recovery process counteracting the process of hardening have not yet been investigated.

---

[29] S. Timoshenko - Strength of Materials, part II, Advanced Theory and Problems, D. van Nostrand Comp.Inc, New York, 1956, p.514

[30] E. Orowan - Proc. Roy. Soc. (London), A, vol 171, p. 79, 1939

8.0 Summary and Conclusions

8.1 *Internal Stress in Creep and Relaxation*

On entering the plastic deformation regime from the more restrained conditions of creep usually two difficulties are encountered, namely unconditional yielding and material hardening. The material properties for creep and plasticity are so remarkably different that initially two different theories were developed, the one for plasticity the other one for creep. Typically the creep law is based on the measured stress σ while the plastic flow rule is based on an excess stress which is the measured stress σ offset by the plastic yield stress σ_p. More recent developments (see eg. ref[31]) showed that plastic straining and creep straining could be combined in one term accounting for an inelastic strain rate. In a unifying approach the inelastic strain rate is based on the measured stress σ, offset by an internal stress variable σ_i which currently is the subject of extensive research work.[32] In the present work the internal stress was defined on a purely mechanical basis.

A test specimen elongated in one direction usually shows contraction in the perpendicular directions. Previous approaches assumed that lateral contraction simply followed the longitudinal elongation movement by means of a prescribed constant ratio. The new proposal is to establish a lateral contraction following more or less independently at an individual rate thereby constituting a variable impedance σ_i to any longitudinal straining. Ultimately a constant value of lateral contraction in the sense of a Poisson's ratio is reestablished. In fact, a lateral stress-strain relationship is defined additionally to the longitudinal one. For the case of a strain hold condition in longitudinal straining the additional relationship is predominantely responsible for stress relaxation. Evidently the properties of the new stress relaxation law can be obtained by appropriate experiments of stress relaxation. The descriptive properties of the combined creep/stress relaxation law were studied and it was found that phenomena such as

- normal primary creep,
- inverted primary creep, both under
  - monotonic and
  - step loading conditions,
- incubation time and anelasticity in stress reduction tests,
- stress relaxation following
  - monotonic and
  - cyclic loading
- recoverable creep

could be reproduced in qualitative agreement with standard types of materials behaviour.

---

[31] E.Krempl, J.J.McMahon, D.Yao - Viscoplasticity Based on Overstress with a Differential Growth Law for the Equilibrium Stress, NASA Symposium, Cleveland, Ohio, June 13-15, 1984

[32] K.P.Walker - Research and Development Program for Nonlinear Structural Modeling with Advanced Time-Temperature Dependent Constitutive Relationship, NASA-Report CR165533, Nov 1981, Figure 8.

8.2 Extrapolation to Plastic Conditions

Incorporating a continuous function of internal back stress σ_i into the creep law does not solve the problem of the rather discontinuous appearance of plastic effects. Also, if in an unifying approach the creep law is used as a vehicle to cross over into the plastic regime, preferably it should not be subjected to additional alterations while being used in such a manner. Therefore the possibilities for establishing extra material properties are narrowed and attention is turned to the only other available term in a Maxwell rheological body, i.e. the term representing the elastic strain. The following characteristic behaviour of the material at the yield point has been postulated.

- If a critical value of creep strain rate $\dot{\varepsilon}_p^c$ is surmounted, the materials internal resistance against deformation partly collapses. More precisely speaking, it is the lateral contraction constraint that is relinquished. A certain amount of lateral strain previously restrained is suddenly released causing a yield strain in longitudinal direction. The yield strain is indistinguishable from elastic straining because like elastic strains the plastic yield strain occurs spontaneously. For this reason the yield strain reduces the elongation of a spring used in a load cell in line with the specimen. It is exactly the internal stress σ_i by which the measured stress is reduced when the corresponding amount of lateral contraction constraint is suddenly released. Consequently, for a mathematical description the term for elastic straining is well suited to absorb a finite amount of spontaneous plastic straining.

Nevertheless, the description of the materials behaviour is not completely satisfactory because in most of the cases the experimental observations reflect a situation during which the measured stress is not spontaneously decreased but rather it is not being increased (ideal plasticity). Therefore it is additionally postulated that:

- In an experiment during which the specimen is subjected to a stress increased at constant rate and controlled by an electronic feed back loop, it is in fact the external work that is continuously applied at the moment when the measured stress appears to be stagnant. Since in a perfectly plastic material no plastic work is done on the yield surface, instead the external work done on the specimen is used internally to remove partly the internal resistance against deformation. To complete the picture the internal back stress does not collapse because of some kind of instability but it is superseded by continuous application of external work. Becoming plastic the material resumes properties more typical for liquids i.e. lateral contraction is entirely dominated by the condition of incompressibility with no lateral contraction constraint imposed. The situation is reminiscent of a similar one encountered in thermodynamics when during the change of the state of aggregate a continuous flow of heat (external work) is required and yet the temperature (measured stress) is not being raised.

  So far in summary the discussion concentrated on only one of the coordinates used in the stress-strain diagram. It is equally important to point out that while the stress remains constant usually the strain rate increases drastically. In a unified approach when all inelastic strains are calculated by a common law this cannot be controlled by the measured stress being stagnant at intervals during which a large increase in strain rate is expected. Therefore, for a continuous increase of strain rate at and above the plasticity limit the controlling quantity was chosen to be a work stress $\bar{\sigma}$ directly derived form the external work done on the specimen. In essence, it has been postulated that the properties of the creep law can be continuously extrapolated into the plastic regime on the basis of a work stress and also on the continuous existence of the internal stress variable σ_i. Other possibilities are conceivable but in the present approach only the measured elastic stress σ was considered to be affected by the collapse of the internal stress σ_i.

Altogether three limit values have been introduced into the present theoretical approach:

- The drag stress K marks off a value of stress above which an increase in effective stress $\bar{\sigma} + \sigma_i$ causes considerably more increase in strain rate than below that value.

- The plastic strain rate yield limit $\dot{\varepsilon}_p^c$ characterizes the transition into the plastic regime by means of the step function S_i.

- The elastic limit of strain rate $\dot{\varepsilon}_h^c$ is a variable limit value separating the elastic strain range from the strain range in which hardening occurs. The hardening process characterized by a plastic Young's modulus E_h was investigated only above the plastic strain rate yield limit $\dot{\varepsilon}_p^c < \dot{\varepsilon}_h^c$ and it is effected by the switch function S_h.

According to the postulated material behaviour a qualitative relationship between the plastic yield stress σ_p and the internal stress σ_i is seen as follows:

- Up to the yield limit the strain rate can be continuously increased on the basis of either a linear increase of measured stress σ or a linear increase of work stress $\bar{\sigma}$, both of which are identical in this region. For a further continuous increase of strain rate based on a linear increase of measured stress σ this has to be reduced by the internal stress σ_i (see Section 7 and equation (31)). Obviously, the necessity for a reduction in stress has been noticed early in the development of flow rules. However, the lack of any characteristic value of stress other than the yield stress σ_p led to the choice of yield stress as a characteristic value of reduction. With reference to the present development the measured stress σ reduced by the internal stress σ_i appears to be a more suitable variable for a steady continuation of strain rate above the yield limit than the measured stress σ reduced by the yield stress σ_p.

A number of numerical tests subsequently listed were performed to compare qualitatively the calculated material behaviour with typical experimental effects.

- A stress-strain relationship was evaluated for a work stress $\bar{\sigma}$ being increased at constant rate and including unloading paths.
- A series of stress-strain curves were calculated for various constant rates in work stress $\bar{\sigma}$, for various constant rates in measured stress σ and for various applied constant strain rates.
- A negative strain rate sensitivity was derived from the set of curves obtained for various applied constant strain rates.
- The effect of isotropic hardening was demonstrated.

8.3 *Perspective Outlook*

The envisaged application of the constitutive equation in the context of Finite-Element calculations for large mechanical components requires a tri-axial mathematical formulation rather than the uni-axial one developed hitherto. At first sight the extension to tri-axiality appears to be more difficult than in the usual case when the rate of volumetric straining is assumed to be zero in order to comply with the incompressibility condition. Such a simplifying assumption is contradictory to the presently introduced concept which allows for a retarded balance prior to a constant volume being reestablished. The introduction of temporary changes in volume attributed to the material behaviour during creep and plastic deformation has far reaching consequences concerning the Finite-Element algorithm:

- Most likely it cannot be avoided that an additional virtual work statement is introduced enforcing the Prandtl-Reuss Equation which relates changes in volume with changes in the hydraulic stress conponent. The problem was outlined by Zienkiewicz.[33]

Also, it should be pointed out that a constitutive equation like the present one capable of producing strain at extremely different rates can cause instability problems in the numerical algorithm used in Finite-Element calculations. The problem has been studied by the authors[34] , and it can be briefly described as follows:

- Local yielding causes stresses to be released locally. The released stresses have to be redistributed globally in order to meet the equilibrium condition of forces within the body. Likewise the mathematical algorithm is split into two parts. Firstly, stresses are released locally and unconditionally by direct use of the constitutive equation which in the present case is extremely non-linear and also non-stationary by nature. Secondly, the stresses released within one time step are then redistributed by solving a linearized system of equations once for each time step, i.e. excluding the more elaborated implicit integration schemes. In the case of a mismatch when more stresses are released per time step than can be redistributed by the linearized numerical algorithm within the same time step, the unbalanced stresses can cause instability. Although the time stepping procedure to a certain degree is self-equilibrating, defection ranges from divergency to small oscillations about the otherwise stationary solution. The problems

---

[33] O.C.Zienkiewicz - Viscous Incompressible Flow with Special Reference to Non-Newtonian (Plastic) Fluids, International Centre for Computer Aided Design, Course on Advanced Topics in Finite Element Analysis, S.Margherita, Italy, June 3-7, 1974, Lecture Series N1/74, p. 158

[34] H.Cords, G.Kleist, R.Zimmermann - Berechnung von Kriechverformungen unter strikter Einhaltung kontinuums-mechanischer Gleichgewichtsbedingungen, Kernforschungsanlage Jülich GmbH, JÜL-Spez-321, Juli 1985, ISSN 0343-7639

grow with the degree of non-linearity of the constitutive equation and also with increasingly non-stationary conditions.

Obviously for the sake of numerical stability a compromise has to be found between the two existing algorithms, the one for creep, the other for plasticity. The algorithm for creep, which introduces small load increases per time step with a subsequent one-step redistribution, has to be supplemented by the algorithm for plasticity, which, with no reference to time, introduces small load increases redistributed for equilibrium employing a complete iteration process.

However, immediate efforts in the development of the described constitutive equation should be directed at a quantitative agreement between calculated and measured data for a number of test cases. With respect to additional fields of application, it is conceivable to complement the set of differential equations in order to account for damage accumulation and effects due to the variable influence of dislocation density.[35]

If it is possible to confirm the present theoretical approach by a number of specifically chosen experiments and if it is possible to show convincingly that the group of effects described in this paper in fact fall into one category, it may be also possible to single out variations from the standardized types of material behaviour which are due to metallurgical effects (precipitation, over ageing, corrosion etc) and eventually to incorporate them into a descriptive formulation.

---

[35] H.Cords, G.Kleist, R.Zimmermann - Development of a Creep Law for Metals at High Temperatures, Transactions of the 8th International Conference on Structural Mechanics in Reactor Technology, Brussels, Belgium, Aug 19-29, 1985, Vol L 6/3 p.287

Appendix A. Complete Set of Formulae for Constitutive Equation

A.1 Set of Simultaneous Differential Equations

$$\dot{\varepsilon}^c = \operatorname{sign}(\bar{\sigma} + \sigma_i)\left|\frac{\bar{\sigma} + \sigma_i}{K}\right|^n \qquad \text{Norton's creep law for inelastic strain rate} \qquad (A1)$$

$$\dot{r} = -r\,\frac{\kappa + \lambda|\dot{\varepsilon}^c|}{1 - \nu\dfrac{\bar{\sigma}}{E}}\,\hat{\dot{\varepsilon}}_{rr} \qquad \text{stress relaxation, definition of a radius function} \qquad (A2)$$

superposition of elastic and inelastic strain rates - *alternative* choice for three load control systems

$$\dot{\varepsilon} = \dot{\varepsilon}^c + \frac{\dot{\sigma}}{\bar{E}} \qquad \text{load controlled by measured stress } \sigma \qquad (A3)$$

$$\dot{\varepsilon} = \dot{\varepsilon}^c + \frac{(2S_t - 1)^2}{2 - (2S_t - 1)^2}\,\frac{\dot{\bar{\sigma}}}{\bar{E}} \qquad \text{load controlled by work stress } \bar{\sigma} \qquad (A4)$$

$$\dot{\sigma}_0 = \bar{E}e^{-\varepsilon^c}(\dot{\varepsilon} - \dot{\varepsilon}^c) - \sigma_0\dot{\varepsilon}^c \qquad \sigma = \sigma_0 e^{\varepsilon^c} \qquad \text{load controlled by total strain } \varepsilon \qquad (A5)$$

A.2 Auxiliary Equations - Definitions

$$\hat{\varepsilon}_{rr} = (1 - \nu\frac{\bar{\sigma}}{E}) - \frac{r_0}{r}e^{-1/2(\bar{\sigma}/E + \varepsilon^c)} \qquad \text{constrained radial strain} \qquad (A6)$$

$$\bar{\sigma} = \sigma - S_t\sigma_i \qquad \text{work stress } \bar{\sigma} \qquad (A7)$$

$$\sigma_i = -\frac{2\nu E\,\hat{\varepsilon}_{rr}}{(1 + \nu)(1 - 2\nu)} \qquad \text{internal back stress } \sigma_i \qquad (A8)$$

$$\bar{E} = (1 - S_h)E + S_h E_h \qquad \text{dual-valued Young's modulus for calculation of elastic strains} \qquad (A9)$$

$$S_h = \frac{1}{4}\{1 + \tanh[\alpha(|\dot{\varepsilon}^c| - \dot{\varepsilon}_h^c)]\}\left\{1 + \tanh\left(\frac{\alpha x}{100}\right)\right\} \qquad \text{definition of hardening range} \qquad (A10)$$

$$\text{with} \quad x = \begin{cases} \sigma\,\dot{\sigma} & \text{if controlled by measured stress} \\ \bar{\sigma}\,\dot{\bar{\sigma}} & \text{if controlled by work stress} \\ \sigma\,(\dot{\varepsilon} - \dot{\varepsilon}^c) & \text{if controlled by strain} \end{cases}$$

$$S_t = \frac{1}{2}\left\{1 + \tanh\left[\frac{2(\sigma + \bar{\sigma} - 2\sigma_p)}{-\sigma_i}\right]\right\} \qquad \text{transitional function between elasticity and plasticity} \qquad (A11)$$

$$\text{with} \quad \sigma_p = K\operatorname{sign}(-\sigma_i)\,|\dot{\varepsilon}_p^c|^{1/n} - \frac{3}{4}\sigma_i \qquad \text{inflection point} \qquad (A12)$$

A.3 Hardening Rule

if $[S_h > 0]$ then $\{\dot{\varepsilon}_t^c = \max(|\dot{\varepsilon}^c|, \dot{\varepsilon}_h^c)\}$ else $\{\dot{\varepsilon}_h^c = \dot{\varepsilon}_t^c\}$ (A13)

A.4 Possibility of Other Load Control Systems

$\varepsilon = \ln|1 + \varepsilon_0|$ control by technical strain ε_0 (A14)

$\varepsilon = \dfrac{\dot{\varepsilon}_0}{1 + \varepsilon_0}$ or technical strain rate $\dot{\varepsilon}_0$ (A15)

$\sigma = \sigma_0 e^{\varepsilon^c}$ control by load stress σ_0 (A16)

$\dot{\sigma} = \dot{\sigma}_0 e^{\varepsilon^c} + \sigma\dot{\varepsilon}^c$ or load stress rate $\dot{\sigma}_0$ (A17)

Appendix B. Nomenclature

E	Young's modulus
E_h	plastic Young's modulus, hardening coefficient
$\overline{E}$	dual-valued Young's modulus
K	drag stress
n	exponent in Norton's creep law
r	current radius of a cylindrical specimen
$\dot{r}$	rate of radial contraction or expansion
r_0	initial radius of the cylindrical specimen
$\dot{r}_g$	rate of radial contraction as approximated by the generator function
t	time
S	strain rate sensitivity
S_t	step function relating measured stress σ with work stress $\overline{\sigma}$
S_h	switch function to delimit the range of hardening
W	total external strain work
W_i	internal strain work
W_p	elastic/plastic strain work
x	variable indicating loading ($x > 0$) or unloading ($x < 0$)
α	promptitude of the switch function S_h
Δr	radial displacement - constrained radial contraction
ε	total longitudinal strain
$\dot{\varepsilon}$	total longitudinal strain rate
ε_0	technical strain
$\dot{\varepsilon}_0$	technical strain rate
ε^c	inelastic strain - creep strain, plastic strain
$\dot{\varepsilon}^c$	inelastic, creep and plastic strain rates

ε^{el}	elastic strain
$\dot{\varepsilon}^{el}$	elastic strain rate
ε_{rr}	radial strain
$\hat{\varepsilon}_{rr}$	constrained radial strain
$\varepsilon_{\theta\theta}$	azimuthal strain - elastic
ε_{zz}	longitudinal strain - elastic
$\dot{\varepsilon}_h^c$	limit for strain hardening
$\dot{\varepsilon}_p^c$	plastic strain rate yield limit
$\dot{\varepsilon}_i^c$	temporarily used for $\dot{\varepsilon}_h^c$
κ	relaxation coefficient
$\tilde{\kappa}$	temporarily used for κ
λ	ductility coefficient
ν	Poisson's ratio
σ	longitudinal stress
$\dot{\sigma}$	longitudinal stress rate
σ_0	load stress - load divided by the initial value of cross section $r_0^2\pi$
$\dot{\sigma}_0$	load stress rate
$\overline{\sigma}_0$	work stress referred to the initial cross section
$\dot{\overline{\sigma}}_0$	work stress rate
σ_i	internal back stress
$\dot{\sigma}_i$	internal back stress rate
σ_p	plastic yield limit - stress at inflection point of the step function S_t
$\overline{\sigma}$	work stress
$\dot{\overline{\sigma}}$	work stress rate
σ_{rr}	radial stress
$\sigma_{i_{rr}}$	internal radial stress
$\sigma_{\theta\theta}$	azimuthal stress
σ_{zz}	longitudinal stress - identical with σ
$\sigma_{i_{zz}}$	internal axial stress, equivalent to σ_i
τ	relaxation time
$\tilde{\tau}$	temporarily used for τ